WIDESPREAD FATIGUE DAMAGE MONITORING - ISSUES AND CONCERNS*

T. SWIFT

Federal Aviation Administration
3229 East Spring Street
Long Beach, CA 90806-2425

ABSTRACT

This paper is intended to illustrate the considerable effect that small in-service undetectable multi-site-damage (MSD) can have on the residual strength capability of aging aircraft structures. In general, very few people in the industry believe that tiny cracks of undetectable size are a problem because they know that many aircraft have been able to survive much larger damage. In fact they have been certified for this large damage capability. However, this is not the issue. The real issue is the effect the tiny cracks, at multiple sites, have on the large damage capability which the industry has become accustomed to expect and which the aircraft have been certified to sustain. The concern is that this message does not appear to be fully undertood by many people outside the fracture community. The prime purpose of this paper, therefore, has been to convey this message by describing in simple terms the net section yielding phenomenon in ductile materials which causes loss in lead crack residual strength in the presence of MSD. The explanation continues with a number of examples on complex stiffened structures, using the results of previous finite element analyses, which illustrate that the effect of MSD is extremely sensitive to structural configuration. It is hoped that those members of the aviation community who believe that tiny cracks are not a problem will read this paper very carefully.

INTRODUCTION

The ALOHA 737 accident in Hawaii on April 28, 1988 created what may be termed a minor "Structural Integrity Revolution" in the Commercial Transport Industry. This minor revolution can, perhaps, be compared to that existing in the fatigue and fracture community in the aftermath of the F-111 accident on December 22, 1969 at Nellis Air Force Base in Nevada. A few weeks after the Aloha accident the Federal Aviation Administration (FAA) sponsored "The International Conference on Aging Airplanes" held in Washington D.C. in June of 1988. Subsequently, in August of 1988, The Airworthiness Assurance Task Force (AATF), later retitled The Airworthiness Assurance Working Group (AAWG), was formed by The Air Transport Association (ATA) of America and The Aerospace Industries Association (AIA) of America. This group, working in cooperation with FAA and other airworthiness authorities, have made significant contributions to improving the airworthiness of the aging fleet of

* Presented at the 5th International Conference on Structural Airworthiness of New and Aging Aircraft, Hamburg, Germany, June 16–18, 1993.

transport airplanes. Among these contributions are model specific reassessments of Supplemental Structural Inspection programs, incorporation of safety related Service Bulletins not previously mandated and the development of mandatory Corrosion Control programs. This activity is now being extended to the Commuter Fleet of airplanes.

Soon after the ALOHA accident the FAA formulated a draft Special Federal Airworthiness Regulation (SFAR) proposing that older airplanes have, as a minimum, one lifetime of fatigue testing beyond the current fleet lead aircraft. The purpose of this rule was to reduce the exposure to unknown fatigue problems and identify multiple-site-damage (MSD) before it occurred in the commercial fleet. In June of 1990 the AATF/AAWG undertook a review of the proposed SFAR and published a report titled "A Report of the AATF on Fatigue Testing and/or Teardown Issues". This report, [1], outlined alternative means to ensure that widespread fatigue damage would not occur in the transport fleet. This was to be achieved through a structural audit of each of the aging fleets of airplanes. With this in mind a Structural Audit Evaluation Task Group (SAETG) was formed under the umbrella of the Aviation Rulemaking Advisory Committee (ARAC) working through the Transport Aircraft and Engine Sub-Committee (TAES). The charter of this task group was to develop a SFAR titled "Widespread Fatigue Damage Evaluation (Aging Aircraft) with a supporting Advisory Circular having the same title. These documents were intended to provide a common set of guidelines to establish the onset of WFD for the aging fleet of commercial transport airplanes. The Structural Audit Evaluation Task Group has been supported by a further activity under the umbrella of AATF/AAWG conducted by the Industry Committee on Widespread Fatigue Damage (ICWFD). The SAETG includes participating members from the airworthiness authorities while the authorities have participated in the ICWFD as observers only. The SFAR and accompanying AC, produced by the SAETG, are intended to initially address eleven fleets of transport aircraft as follows:- B707/720, 727, 737 (100 and 200 models only), 747 (100 and 200 models only), BAE 1-11, DC-8, DC-9, DC-10, F28, A-300 (B2, B4-100, B4-200, C4 and F4 models only)2 and L-1011.

As can be seen from this introduction major steps have been taken by the so called "Three Legged Stool" (manufacturers, operators and authorities) to improve the structural airworthiness of the aging fleet of airplanes. Notwithstanding this considerable effort there are still outstanding issues and concerns related to the formulation of WFD which is believed to have been a contributing factor in the probable cause of the ALOHA 737 accident.

DEFINITIONS

The two industry activities SAETG and ICWFD, the AIA Structures Technical Subcommittee and the Technical Oversight Group Aging Aircraft (TOGAA) have expended considerable effort defining Widespread Fatigue Damage (WFD) and its two subsets Multiple Site Damage (MSD) and Multiple Element Damage (MED). The definitions

agreed by these groups are:-

Widespread Fatigue Damage (WFD) in a structure is characterized by the simultaneous presence of cracks at multiple structural details that are of sufficient size and density whereby the structure will no longer meet its damage tolerance requirements (e.g., not maintaining required residual strength after partial structural failure).

Multiple Site Damage (MSD) is a type of Widespread Fatigue Damage characterized by the simultaneous presence of fatigue cracks in the same structural element (e.g., fatigue cracks that may coalesce with or without other damage leading to a loss of required residual strength).

Multiple Element Damage (MED) is a type of Widespread Fatigue Damage characterized by the simultaneous presence of fatigue cracks in similar adjacent structural elements.

A further definition for Widespread Fatigue Damage has been proposed by Professor Jim Mar, Chairman of TOGAA. Professor Mar simulates WFD to AIDS in humans. It is a point in the life of an aircraft when the immune system (in this case fail safe or damage tolerance capability) starts to deteriorate. Because WFD in the form of MSD can drastically affect certified levels of residual strength, even when it is so small it is in-service non detectable, Professor Mar believes that either MSD exists or it doesn't. There is nothing in between that can be managed by inspection. Unlike AIDS, however, MSD can be cured by reliably predicting when it is likely to degrade residual strength capability below required levels using the best tools currently available and then modifying the structure in ample time before it has a chance to deteriorate the immune system.

PRIMARY ISSUES AND CONCERNS

As previously mentioned the SAETG supported by the ICWFD are in the process of establishing guidelines to estimate the onset of WFD. It is the intention that the manufacturers provide this estimate based on their knowledge of background fatigue testing and stress analysis of the aircraft. However, the operators have made it clear that they will be reluctant to allocate funds for aircraft modification unless they are sure the estimate is correct. Bearing this in mind the ICWFD has proposed a monitoring period between the first anticipated cracking indications and the onset of WFD where special inspections will be performed of susceptible areas with a view to escalating the manufacturers' estimate of WFD. This monitoring period is illustrated in Figure 1.

Since the ALOHA accident it has been the contention of the airworthiness authorities that managing structural safety in the presence of WFD or MSD is not reliable with current in-service inspection sensitivity. In fact, the FAA no longer allows continued inspection of known problem areas as an alternative to fixing the

problem itself. The issue is, then, how can the monitoring period be technically viable when MSD cannot be reliably found before it has already reduced residual strength capability below regulatory levels.

The concern appears to be confined to just a few people who fully understand the implications of MSD. The others appear to think that small MSD can never be a problem because they have been able to tolerate much larger cracks in the past. This is true but this is not the issue. The issue is that the airplane is designed to tolerate certain lead crack sizes. The inspection program is based on these lead crack sizes and MSD has significant effect on residual strength at these sizes. Further to this the airplane is also designed to sustain a certain degree of discrete source damage due to engine disintegration and other possible sources. MSD can also degrade this discrete source damage capability. It has been pointed out to the operators that the monitoring period will not include "business as usual" inspections but will require finding cracks far below the threshold capability of current Non Destructive Inspection (NDI) used in service. They have chuckled amongst themselves at this and commented that they will need to carry pocket electron microscopes with which to perform the inspections. The truth is that this is what may be required in some areas if the initial estimate made by the manufacturers is to be escalated based on inspections performed during the monitoring period.

It has been stated many times that structure can be made to operate forever with proper inspection and maintenance. The damage tolerance philosophy is supposed to find damage before catastrophe. However, in-service inspections based on a damage tolerance philosophy are designed to find a single lead crack in a structure which is not expected to crack under normal circumstances but may crack within the service life due to initial manufacturing or in-service induced accidental damage. Damage tolerance was not intended as a safety management tool for structures operating beyond their initial design life goals or beyond the point where WFD is likely to occur.

Since the ALOHA accident a large number of researchers have been concerned with predicting the growth of MSD to link-up for what appears to be an endless range of cracking scenarios. This is apparently being considered with a view to managing safety in the presence of MSD. The truth is the range of scenarios <u>is</u> endless, it is impossible to consider all cracking scenarios and it is too late to control when it becomes inspectable.

This author became concerned about the implications of MSD in the early days of the DC-10 development test program in the late sixties where many components were tested to many times the design life goal of the airplane. This concern was expressed in reference [2], presented in Toulouse in May, 1983, where the difficulties of inspecting for MSD and the net section yielding phenomena were pointed out.

Further concerns were expressed in reference [3], presented in Pisa in May, 1985. Reference [3] outlined the fact that residual strength of specimens containing small cracks in 2024-T3 material was limited by typical net section yield stress. That paper also warned that although 2024-T3 material was the most superior alloy for large damage capability its capacity to withstand MSD was limited by low yield strength of the material. Reference [3] also warned that lead crack residual strength could be influenced by fastener holes ahead of the lead crack tip due to plastic yielding between the lead crack tip and the holes. It was pointed out that all residual strength tests performed so far did not consider this phenomenon.

Reference [4] presented in Ottawa in June, 1987, warned that the formulation of MSD may prevent skin "Flapping", a so called safe decompression phenomenon, being depended upon to eliminate the need to perform detailed inspections of lap splices.

As recently as a year ago an explosive decompression failure occurred in the fuselage on a full scale test specimen in Europe. This failure came as a complete surprise to structural engineers who were aware that MSD existed in a lap splice but who were unaware of the serious implications of MSD.

An attempt was made in reference [5] to illustrate the effects of MSD on lead crack residual strength. This paper was, however, presented to a select audience of fatigue specialists at Delft University who it is believed fully understood the implications. However reference [5] is probably not widely publicized among the airline community. At the risk of being criticized for duplication much of the material in reference [5] is again repeated here with the hope that the issues and concerns related to this dreaded disease in aging airframes outlined above will be better understood by a wider audience.

EFFECTS OF WFD/MSD/MFD ON DAMAGE TOLERANCE PHILOSOPHY

The philosophy of damage tolerance assures structural integrity through in-service directed inspections of critical structure. As mentioned earlier the airplane is designed not to crack within one lifetime but may crack due to damage caused during manufacture or during service. The inspection threshold and frequency is determined by engineering evaluation considering the aircraft utilization, material crack growth rates and residual strength capability. A stress spectrum is derived for each principal structural element (PSE) and a safe crack growth period is calculated starting with a single lead crack of a size that is considered to be detectable in-service with a high degree of reliability and confidence and ending with the critical crack size at limit load. This is illustrated by Figure 2. The safe crack growth period is normally divided by a factor of either 2 or 3

depending upon the type of structure. The safety of the airplane depends upon finding cracks before they reach a critical length. The residual strength calculation, supported by tests, normally does not assume the presence of MSD because the airplane is supposed to be designed so that WFD will not occur within the design life goal. However, now that many aircraft are operating beyond this goal the possibility that WFD will occur increases with time. If WFD does occur it can drastically affect the residual strength capability of the single lead crack at limit load. This is illustrated by Figure 3 which shows a typical residual strength diagram for a single lead crack indicated by the upper curve. The lower curve illustrates the effect of MSD ahead of the lead crack tip. As can be seen the effect of the MSD cracks is to decrease the critical crack size at limit load or to decrease the residual strength capability. The effect of decreasing the critical crack size is illustrated by Figure 4. As can be seen this causes a reduction of the safe crack growth period resulting in a much shorter required inspection frequency.

A particularly difficult issue to deal with is the effect of MSD on the discrete source damage capability of the pressure cabin. The airplane is normally designed to sustain damage from discrete sources such as from engine fragments during disintegration. Usually the pressure cabin is certified to a certain level of damage substantiated by discrete source damage tests. For example, in the case of damage from an engine disc fragment, a harpoon blade simulating the disc fragment is fired into the pressurized cabin. This is illustrated by Figure 5. An example of these tests is further illustrated by Figures 24, 25 and 26 of reference [4] for the DC-8 fuselage. Continued operation of the airplane beyond the initial design life goal increases the probability that WFD in the form of MSD will occur in the pressure cabin thus degrading the discrete source damage capability.

As mentioned earlier it is difficult for the layman to appreciate the consequences of extremely small cracks of less than detectable size because aircraft have been able to sustain much larger cracks in the past. However, these extremely small cracks, which develop and become widespread with extended use of the aircraft, have the ability to drastically reduce this large crack residual strength capability which is expected to exist.

EFFECT OF MSD ON LEAD CRACK RESIDUAL STRENGTH

The residual strength of unstiffened panels containing lead cracks can be determined using conventional fracture mechanics principles. For an infinitely wide thin sheet panel the residual strength can be expressed as:

$$\sigma_R = K_c/\sqrt{\pi a} \qquad [1]$$

The value of K_c is the plane stress fracture toughness of the material obtained from unstiffened cracked panel tests and a is half the crack length. For 2024-T3 material, the most common alloy

used for fuselage skins, the full plane stress fracture toughness is not achieved unless the panel width is greater than 50 inches. If critical stress intensity factor is calculated from test results of panels narrower than 50 inches then the resulting values, limited by yielding of the intact ligament on each side of the crack, will be lower than the plane stress fracture toughness. This effect is illustrated by Figure 6 which shows critical stress intensity factor as a function of panel width determined from test results, references[6]and [7]. It can be seen that for panels with widths less than 50 inches the critical stress intensity factor is limited by ligament yielding. This means that failure of 2024-T3 panels with widths less than 50 inches will be governed by net section yielding rather than by stress intensity factors reaching a critical value.

The fracture strength of most aluminum alloys is limited to the typical net section yield strength of the alloy. This phenomenon is best illustrated by considering test results for specimens containing small cracks. Figure 7 shows data for 2024-T351 plate, reference [3], and indicates failure stresses equal to the typical yield strengths for unnotched specimens from the same batch of material. These yield strengths are based on the 0.2% offset strain. Test point A represents a data point for a specimen with an uncracked hole which failed at 59.5 KSI. When this point is compared to the unnotched typical ultimate strength of 73 KSI it is evident that the material is severely notch sensitive, ie., a loss in strength of 18½%.

Feddersen in reference [8] suggested a residual strength criterion for center cracked panels as shown by Figure 8. A residual strength curve is plotted based on $K_c/\sqrt{\pi a}$ or the fracture mechanics mode of failure. A line is drawn from point A, representing typical tension yield strength, tangent to the $K_c/\sqrt{\pi a}$ curve at point B which is at 2/3 the material yield strength. A second line is drawn from point D representing panel width W which in the example shown is 50 inches, tangent to the curve shown by point C, which is at one third the panel width. The residual strength curve is represented by line ABCD. Residual strength is governed by fracture mechanics only between B and C. As illustrated in reference [8] test data falls on this line. For narrower panels fracture is governed by the lines indicated for panel widths W_1, W_2, W_3 and W_4.

For the MSD case shown on Figure 8 the effective panel width is the fastener spacing P or W_1. The residual strength for this case, according to the Feddersen method, is given by the line A W_1. The equation for this line would then be:-

$$\text{Residual Strength } \sigma_R = F_{ty}[P-2a]/P \qquad [2]$$

Where F_{ty} is the typical yield strength, P is the fastener spacing and 2a is the total length of the crack from tip to tip.

Based on this information it appears reasonable to assume that link-up of a lead crack with an MSD crack would occur when the

intact ligament stress between the lead crack tip and the MSD crack tip reached the typical yield strength of the material. This leads one to the intuitive link-up criterion illustrated by Figure 52 of reference [4] and again restated in Figure 21 of reference [5]. As mentioned earlier in this paper it is not clear that the effects of MSD on lead crack residual strength are fully understood by very many people of authority. So this concept will again be repeated in the hope that the old British saying, "Third Time Does It", will apply. Figure 9 restates the link-up criterion. The lead crack plastic zone size R_2 can be calculated using one of the many plastic zone models in the literature. Similarly the MSD crack plastic zone R_1 can be calculated. The interaction between the two crack tips can be determined from Figures 75 and 76 of reference [10]. As the remote stress level increases the plastic zone sizes will increase and it is suggested that the two cracks will link-up when the two plastic zones touch each other as indicated in Figure 9. Thus the entire ligament between the two crack tips has yielded. The net stress at link-up appears to be controversial. As mentioned earlier intuition supported by a considerable background of testing suggests this should be in the neighborhood of the yield stress. It is not yet fully understood whether this is at the 0.1% or the 0.2% offset strain or at some other strain.

Under FAA funded research conducted soon after the ALOHA accident it was determined that the net section stress at failure for 8 inch and 4 inch wide 2024-T3 specimens 0.04 inches thick containing MSD cracks was at least equivalent to the flow stress or approximately $[F_{tu} + F_{ty}]/2$, reference [9]. The flow stress quoted in this case was 65 KSI.

In reference [5] this author used the Irwin plastic zone model with an estimated link-up stress of 50 KSI to illustrate the loss in lead crack residual strength in the presence of MSD. The Irwin plastic zone model does not satisfy equilibrium as pointed out in reference [11]. There are a number of plastic zone models available but not much evidence yet to show that one is better than another.

Other research, reference [12], conducted by CDR Jim Moukawsher of the USCG at Purdue University on 2024-T3 panels 9 inches wide and 0.09 inches thick containing lead cracks under the influence of MSD cracks indicates reasonably good correlation with this link-up criterion using the Irwin plastic zone model and the 0.1% offset yield strength. For these panels this value was 51 KSI.

Research is being conducted under FAA funding to establish a sound link-up criterion. For the purposes of this paper the Irwin plastic zone model combined with a link-up stress of 50 KSI will be used. It is the purpose of this paper to attract more attention and to convince the airline industry of the problem of loss in lead crack strength in the presence of MSD rather than to establish an exact analytical method. It is hoped that this will be achieved in the near future by FAA funded research.

Figure 9 illustrates the intuitive link-up criterion and shows a

lead crack of half length a_2 which has been propagating along a row of holes. A hole containing a MSD crack exists ahead of the lead crack tip. Link-up of the MSD crack with the lead crack will occur when the lead crack plastic zone R_2 touches the MSD plastic zone R_1 as shown in the figure, ie.,

$$R_1 + R_2 = [P-d/2-a_1] \qquad [3]$$

Plastic zone sizes based on the Irwin model are:

$$R_1 = [K_1/\sigma_y]^2/[2\pi] \qquad R_2 = [K_2/\sigma_y]^2/[2\pi]$$

$$K_1 = \beta_h\beta_{I1}\sigma[\pi a_1]^{1/2} \qquad K_2 = \beta_s\beta_{I2}\sigma[\pi a_2]^{1/2}$$

Therefore:

$$[(\beta_h)^2(\beta_{I1})^2\sigma^2\pi a_1 + (\beta_s)^2(\beta_{I2})^2\sigma^2\pi a_2]/(2\pi\sigma_y^2) = P-d/2-a_1$$

Therefore:

$$\sigma_R = \{2\sigma_y^2(P-d/2-a_1)/[\beta_h^2\beta_{I1}^2a_1 + \beta_s^2\beta_{I2}^2a_2]\}^{1/2} \qquad [4]$$

Where:

σ_R = Remote gross stress which causes the plastic zones to touch.

σ_y = Local stress causing link-up. Approx. equal to flow stress or $[F_{tu} + F_{ty}]/2$. (50 KSI assumed in this paper)

β_h = Bowie Factor ref. [13] for cracks at a hole but normalized to crack length measured from hole 1 center, ie., a_1. (see example below).

β_{I1} = Geometric correction factor for crack 1 tip due interaction with lead crack 2. This is determined from reference [10] Figure 75 based on an equivalent lead crack 2 length $a_{e2} = \beta_{s2}^2a_2$ and an equivalent crack 1 length $a_{e1} = \beta_h^2a_1$; ie., it is assumed that the effect of one crack on the other is due to interacting Ks. Equivalent crack lengths are used to calculate interaction accounting for individual crack Ks. This effective crack length philosophy, used here to account for effects of stiffening elements on K, needs further validation.

β_s = Geometric correction factor for lead crack 2. This factor would include the effects of stiffening or any edge effects.

β_{I2} = Geometric correction factor for crack 2 due to interaction of crack 1. This is determined from reference [10] Figure 76 based on an equivalent lead crack 2 length $a_{e2} = \beta_{s2}^2a_2$ and equivalent crack 1 length $a_{e1} = \beta_h^2a_1$.

Consider the MSD cracks in hole 1 of Figure 9 are 0.05 inches at each side of the hole. Assume the hole diameter is 0.19 inches so that $a_1 = 0.145$ inches. The stress intensity factor for two cracks at a hole under uniaxial loading is given as $K = [\pi L]^{1/2}F(L/r)$ in reference [13] where L is the crack length and r the hole radius. At a value of $L/r = 0.05/0.095$, $F(L/r) = 1.8$ [by plotting L/r versus F(L/r)]. The value of β_h can then be obtained as follows:

$$\beta_h = [1.8^2(0.05)/0.145]^{1/2} = 1.057$$

SIMPLE UNSTIFFENED PANEL EXAMPLES

In order to illustrate the link-up phenomenon a simple case of a lead crack in an infinitely wide 2024-T3 unstiffened panel is shown in Figure 10. The curve ABEF represents the residual strength for the lead crack alone uninfluenced by any MSD and is simply based on equation 1 with the plane stress fracture toughness K_c assumed to be 150 KSI $\sqrt{IN}$. Now assume that a pair of 0.19 inch diameter holes containing 0.05 inch long MSD cracks are located ahead of the lead crack tips each at a distance 8 inches from the panel center line as shown on Figure 10. Line HBC is a plot of stress σ_R as a function of lead crack half length a_2 which will cause link-up of the MSD crack with the lead crack tip. Line HBC is based on equation 4 with $\beta_s = 1.0$ for the infinite wide unstiffened panel. The term $(P-d/2-a_1)$ in equation 4 is replaced by L, the distance between the lead crack tip and the MSD crack tip.

Therefore: $$\sigma_R = \{2\sigma_y L/[\beta_h^2\beta_{11}^2 a_1 + \beta_s^2\beta_{12}^2 a_2]\}^{1/2} \qquad [5]$$

For this example $\beta_h = 1.057$, σ_y is assumed 50 KSI, β_{11} and β_{12} are obtained from reference 10 Figures 75 and 76 respectively. Referring to Figure 10, imagine this panel in a tensile testing machine with lead crack half length equal to a_{EX} as shown on Figure 10. If the remote stress applied to the panel is increased to σ_{EX} corresponding to point J then link-up of the MSD crack with the lead crack will occur and the effective lead crack length will suddenly increase to point K but will still be stable. The remote stress can now be increased to point E when fast fracture and failure will occur. It can be seen on Figure 10 that the residual strength for lead cracks beyond point B will be reduced to point E.

Now consider two pairs of 0.19 inch diameter holes containing 0.05 inch long MSD cracks at distances 8 and 9 inches from the panel center line as shown on Figure 11. Again line ABGH represents the residual strength for the lead crack uninfluenced by MSD. Line LBC is a plot of remote stress σ_R as a function of lead crack half length a_2 which will cause link-up of the MSD crack, centered at 8 inches from the panel center line, with the lead crack tip. Similarly, line ME is a plot of remote stress σ_R which will cause link-up with the second MSD crack centered at 9 inches from the panel center line. Lines LBC and ME are based on equation 5. Referring to Figure 11, again imagine the panel is in a tensile testing

machine with lead crack length equal to a_{EX}. If the remote stress is increased to σ_{EX} then the MSD crack located at 8 inches will suddenly link-up with the lead crack at point J. The lead crack will now be of half length given by point K and will be stable at remote stress σ_{EX}. If the remote stress is again increased the second MSD crack located at 9 inches will link up with the new lead crack at point E which will suddenly extend to point F. The lead crack will remain stable at this stress. If now the remote stress is increased to point G fast fracture will occur and the panel will fail. Figure 11 illustrates that residual strength of lead cracks beyond point B will be reduced to point G under the influence of the two MSD cracks.

Following this process, Figure 12 illustrates the case when several MSD cracks are located ahead of the lead crack tip. In the example shown five MSD cracked holes were considered. It can be seen that the lead crack does not arrest in a hole which would allow a higher stress to be applied up to curve ABG with no MSD at half lead crack lengths beyond B and stress levels higher than E. For lead cracks with lengths beyond point B the residual strength is reduced to a stress no higher than point E.

The analysis developed to plot Figure 12 was repeated with MSD crack lengths 0.01 inches. The resulting residual strength diagram is shown on Figure 13. The loss in residual strength is not as great as shown by Figure 12 for 0.05 inch MSD cracks but is still substantial as indicated by the drop from point B to point E. It must be remembered that even though the MSD crack of 0.01 inch assumed for this example appears very small it occurs at a fastener hole so the effective length of the crack is 2(0.01) + diameter of the hole in addition to any geometrical effects of the hole itself.

It can be seen from these simple examples of unstiffened panels that extremely small MSD cracks of a size that would be in-service non inspectable could reduce the residual strength of lead cracks used in the evaluation to certify the aircraft. However each area of the aircraft, susceptible to MSD, would need to be reviewed to determine the size of MSD that would reduce the residual strength capability below certification limits.

LARGE DAMAGE SIZE SUBSTANTIATION

Many of the aging fleet of transport aircraft, designed prior to amendment 45 of FAR 25.571, were substantiated for large damage capability. Figure 14 illustrates typical fuselage damage sizes substantiated by both analysis and testing. The example shown happens to be for the DC-10 aircraft (Figure 32 of reference [4]) but other aircraft are capable of similar damage. These damage sizes were used for substantiation of the aircraft to the certifying authorities and also used to market the aircraft to the airlines. The subsequent maintenance and inspection programs reflected a certain level of confidence which directly related to this large damage capability. Without this confidence the inspection program may have been much more demanding in terms of

inspection reliability requirements. As the airplanes age, beyond the time which can be substantiated by fatigue testing, the probability that these damage sizes can be retained at the required load levels will diminish with time. Thus, the fairly comfortable feeling enjoyed by the authorities and the flying public created by this large damage capability will also diminish with time. The manufacturers, having all the design data at their disposal, need to establish the point in the life of the aircraft at which the residual strength at these damage sizes will diminish below the required levels. It is believed this can be done with existing evaluation methods.

COMPLEX STIFFENED FUSELAGE STRUCTURE

The methods used to illustrate the considerable effect of MSD on simple unstiffened panels can be extended to complex stiffened structures. Conventional finite element analyses, normally used to calculate stress intensity factors for stiffened structures, can be used to calculate the term β_s in equation 4. A typical finite element idealization, used to calculate the stress intensity factor and stiffener stresses for the case of a longitudinal crack in a fuselage panel, is shown in Figure 15. This analysis is described in more detail in references [14] and [15]. As illustrated in Figure 15 loads are applied to the top of the panel and reactions at the bottom are disconnected one at a time to simulate the propagating crack. The center frame reactions can also be disconnected to represent a broken frame. The effect of stiffening on the crack tip stress intensity factor is obtained by analysis of the unstiffened panel and again of the stiffened panel. The value of β_s is determined by taking a ratio between the stiffened panel and the unstiffened panel crack tip stresses. Crack tip stresses are considered to be the stresses in the last bar still connected to a reaction as shown in Figure 15. The stress intensity factor K for a lead crack can therefore be calculated for a particular fuselage design. The effect of MSD on the residual strength of this lead crack can be determined through the use of equation 4. For a longitudinal crack case in a pressurized cabin equation 4 in this paper can be modified to include the effects of bulging due to pressure by including an additional bulging factor β_B as shown in equation 4 of reference 5.

DISCRETE SOURCE DAMAGE CASE

As an example, let us first consider a pressurized fuselage panel subjected to discrete source damage. Figure 14 shows this damage size for one aircraft type. Figure 5 illustrates testing normally performed to satisfy the requirements of FAR 25.571 paragraph (e), Damage Tolerance (discrete source) evaluation. Harpoon blades, simulating engine disc fragments, are fired into the pressurized and loaded fuselage. This testing is performed to verify that explosive decompression will be prevented in the event the fuselage sustains damage from a disintegrating engine. Examples of the result of this type of testing are shown in reference [4] for the DC-8 aircraft. As the aircraft ages, particularly beyond the life

substantiated by fatigue testing, the possibility exists that MSD may reduce the residual strength capability demonstrated during certification. The size of MSD which can degrade the residual strength below the certified level will depend on the structural configuration. For example, Figure 16 shows two different fuselage circumferential frame designs. Both of these designs are typical of transport aircraft in service today. One has a titanium crack stopper strap and the other does not. Reference [14] contains the results of finite element analysis which can be used to illustrate the differences in these two design concepts.

The frame cross sections for these two typical examples are shown in Figure 17. The sections were idealized as shown. The idealized areas were chosen to simulate the frame cross sectional area and bending moment of inertia. The idealization on the left considers the case with a 0.025 inch thick titanium crack stopper strap 3.0 inches wide with 3, 3/16 inch diameter rivet holes across the section. The idealization for this element was simulated by an equivalent aluminum area of 0.1035 square inches as shown. The frame for this design concept was idealized by the two elements shown which were equal to the total frame area and set in a location to simulate the bending section properties of the frame. The idealization for the frame without the crack stopper strap is shown to the right in Figure 17. In this case the frame was idealized by three elements as shown.

One of the most important considerations in this analytical method is the correct simulation of the flexibility of the load path from the cracked skin into the frame member. Figure 18 shows how this shear path was idealized for the panels described in reference [14]. The diagram to the left shows the shear clip to frame rivet flexibility represented by springs having the same stiffness as the rivets. A shear panel of length b and height h_1 represents the portion of the shear clip above the longeron cutout. The shear panel of length b_2 and height h_2 represents the portion of the shear clip between the longeron cutouts. The shear flexibility of this system is calculated and simulated to a single shear panel B shown to the right of Figure 18. The thickness of this shear panel is calculated to give the same flexibility as the system to the left. Equations used to make this equivalence are shown in reference [15].

The residual strength of a cracked stiffened panel from a skin fracture viewpoint is given by:

$$\sigma_R = K_c/[(\pi a)^{1/2}\beta_S\beta_B] \qquad (6)$$

Where K_c is the skin material plane stress fracture toughness assumed to be 158 KSI $\sqrt{IN}$ for 2024-T3 for this example, β_S is the effect of geometrical elements such as frames, a is half the crack length and β_B is a geometrical effect caused by crack tip bulging due to pressure and shell radius. Since all of the stiffening material at the center of the crack is assumed failed for the discrete damage case the bulging effect has been assumed to behave

like a one bay crack with the bay equal to two frame spacings. The term β_B used here is based on Paul Kuhn's unstiffened shell data [16] together with a cosine function to damp out the bulging as the crack tip approaches the intact frame. The bulging factor used for this analysis was suggested by Prof. Dr. Lüder Schwarmann [17]. The resulting term is:

$$\beta_B = 1+5(2a)/R[\text{Cos}(\pi a/P] \quad (7)$$

Where a = half crack length
R = shell radius
P = frame spacing

Values of the term β_S, for the frame with crack stopper configuration shown in Figure 17, can be obtained from case 5 on page 180 of reference [14]. The values are given in terms of R_{ct} which is the reciprocal of β_S. The critical stiffening element will be the outer crack stopper. Values of the stress concentration factor for the outer crack stopper are also given as σ_{ocs}/σ for case 5 in reference [14]. However, the gross applied stress σ used to calculate the allowable crack stopper stress should only be based on the skin hoop stress whereas in the case of the skin fracture criterion it is usual to consider the principal stress calculated from the effects of hoop stress and skin shear due to fuselage bending. For the example shown here the skin shear is assumed to correspond to a 1.5g fuselage down bending case and is assumed to be 7.37 KSI. The hoop stress corresponds to 82% PR/t and is assumed to be 12.45 KSI. The principal stress is therefore 15.872 KSI. The ratio between the hoop stress and the shear stress is 0.7844. For purposes of plotting a residual strength curve in the usual way the curve is plotted in terms of principal stress when considering the skin fracture criterion. This is slightly conservative because the principal stress acts at an angle but barrel tests [14] have indicated the conservatism is not great. However, the crack stopper stress is only a function of hoop stress so the crack stopper allowable stress at any one crack length is divided by the ratio of 0.7844 to obtain the corresponding principal stress. This is done solely to plot the crack stopper allowable on the same diagram as the skin fracture criterion. The residual strength from a skin fracture viewpoint is calculated in Table 1. As mentioned previously β_S values are obtained from case 5 of reference [14] and β_B is obtained from equation 7.

The residual strength for the configuration with frames without crack stoppers, as shown to the right of Figures 16 and 17, is calculated in Table 2. The finite element analysis results used for this configuration were taken from Case 1 of reference [2] and modified to include the effects of a broken central frame. The results of these two analyses are compared on Figure 19. For the configuration with crack stoppers the residual strength for the two bay crack condition is given by point B which is at the intersection of the skin fracture and outer crack stopper strength curves. Any fast fracture of the skin crack below point B would be arrested. Any fast fracture above B would not be arrested and

complete failure would be precipitated by outer crack stopper failure. The allowable from a skin fracture viewpoint alone is given by point C. In the case of frames without a crack stopper the residual strength is given by point A at the peak of the skin fracture curve. In this case the frame outer cap stress is low enough to cause the allowable from a frame strength viewpoint to be well above the skin fracture allowable.The reason for this is that the load path from the cracked skin into the frame element is extremely flexible as indicated on Figure 18. The frame acting alone is not as effective as the configuration with crack stoppers and this is illustrated by a comparison of the two peaks of the two fracture curves at points A and C. As in the case of the crack stopper, the frame allowable has been increased by dividing by 0.7844. Again, this is done solely to be able to plot the allowable frame stress on the same diagram as the skin fracture criterion. The frame is only loaded from the effects of hoop stress due to cabin pressure whereas the skin fracture criterion is influenced also by skin shear resulting in a skin principal stress. Figure 19 illustrates that both configurations have crack arrest capability at the typical 1.5g plus 82% PR/t stress expected during the discrete source damage event.

Suppose now the aircraft has aged to the extent that MSD has started to form in the skin at fastener holes. Suppose also that stiffener to skin rivet spacing in a longitudial direction, either a skin splice or at a longeron to skin attachment, is 1.25 inches. During the discrete source damage event assume skin ripping has taken place creating a simulated lead crack with fastener holes containing MSD ahead of this simulated lead crack. In other words suppose discrete source damage has occurred to a structure already damaged by fatigue created by utilization beyond the time supported by fatigue test. The effect of this MSD on the residual strength is illustrated by Figure 20 for the configuration of frames with crack stoppers. The effect of various MSD crack sizes on the skin fracture curve is illustrated. The assumption made here in order to illustrate this effect is that there is always a MSD crack centered 1.25 inches ahead of the lead crack tip. This is a reasonable assumption if the lead crack is propagating along a row of fastener holes. The residual strength is given by points B, C and D for MSD crack sizes 0.05, 0.10 and 0.15 inch respectively. The three curves showing the effect of MSD on skin fracture are based on equation 4 which was modified to include the effects of bulging at the lead crack tip given by equation 7. The resulting modified equation is:

$$\sigma_R = \{2\sigma_y^2(P-d/2-a_1)/[\beta_h^2\beta_{I1}^2a_1 + (\beta_s\beta_B)^2\beta_{I2}^2a_2]\}^{1/2} \qquad (8)$$

The calculation for the configuration with crack stoppers and 0.05 inch MSD cracks is shown in Table 3 as an example. The calculation for the other two MSD cracks is similar. Figure 20 illustrates that even though a considerable loss in residual strength due to MSD occurs as indicated by points B, C and D compared to A the configuration with titanium crack stoppers can tolerate a certain amount of MSD. This is shown by comparing the residual strength at

points B, C and D with the applied principal stress level. The calculation for the configuration without crack stoppers is shown in Table 4 for MSD crack sizes 0.05 inch. The calculation for the other two crack sizes is similar. The effect of MSD for the configuration of frames without crack stoppers is shown on Figure 21. Assuming the skin crack arresting frame member is uncracked its allowable is well above the skin fracture curves. The effect of MSD on skin fracture is shown by the three curves whose peaks are at points B, C and D for MSD cracks 0.05, 0.1 and 0.15 inches respectively. Figure 21 illustrates that 0.05 MSD cracks reduce the residual strength down to just above the required value while 0.1 inch MSD cracks and greater cause the residual strength to drop below the required principal stress.

The calculations made reflect a considerable loss in residual strength with even extremely small cracks and the sensitivity to actual MSD crack sizes appears to diminish to some extent. However, the longitudinal fastener spacing appears to have considerable influence on the resulting residual strength. In order to illustrate this the exercise was repeated for a rivet spacing of 1.0 inches. This is a realistic longitudinal rivet pitch for typical transport aircraft fuselage structure. The calculation for the case with crack stoppers is shown in Table 5 for 0.05 inch MSD cracks and 1.0 inch rivet spacing. For frames without crack stoppers the calculation is made in Table 6 for 0.05 inch MSD. As before the calculations for the other MSD crack sizes are similar. Figure 22 shows the results in the case of frames with crack stoppers. As before a considerable loss in residual strength is shown for the three MSD crack sizes but the allowables for the two bay crack case given by points B, C and D are still above the applied principal stress. These points are shown compared to point A which illustrates the residual strength with no effect of MSD.

For the case with no crack stoppers the original residual strength with no effect of MSD is given by point A on Figure 23 which is above the applied principal stress. However, for all the MSD crack sizes considered from 0.05 to 0.15 inches the allowable for the two bay crack case is below the applied principal stress.

It can be seen from these examples that the size of MSD which could degrade the residual strength capability below the required level is very much influenced by the structural configuration. In some cases the monitoring period, defined in Figure 1, may be useful to verify the onset of WFD because the MSD crack sizes may be in-service inspectable. On the other hand there may be some structural configurations where the residual strength has already become degraded below the required residual strength levels before the MSD is in-service inspectable. In these cases the operators will have a tough time convincing the authorities that the initial manufacturers' estimate of the onset of WFD can be escalated. Figure 24 illustrates that for the case without crack stoppers MSD in the order of 0.032 inches would need to be found to prevent the residual strength from being degraded below the required value.

A school of thought exists that the effect of MSD on the residual strength capability of the pressurized fuselage in the event of discrete source damage from engine disintegration can be managed by risk assessment. The Joint Airworthiness Regulations JAR ACJ No. 2 to JAR 25.903 (d)(1) outlines procedures to minimize the risk in the event damage is sustained by a disc fragment. An evaluation should show that there is more than a 1 in 20 chance of catastrophe created by a one third piece of disc plus one third the height of a blade. This is normally done by limiting the sum of the risk angles to 360/20 = 18 degrees as illustrated by Figure 25. Each critical system and structural element is evaluated and a risk angle θ determined for each. For example, Figure 25 identifies a critical system A the loss of which would cause catastrophic loss of the aircraft. If the loss of this system would occur with disc fragment trajectory between θ_1 and θ_2 then θ_A is the critical risk angle for system A. The sum of all the risk angles including systems and structures should be less than or equal to 18 degrees. However, this procedure does not eliminate the need to consider the effects of MSD on longitudinal damage. If in fact longitudinal damage cannot be contained then the structural angle of risk may already be above the 18 degree limit. This is illustrated by Figure 26 which shows that if the fuselage were pierced between angles θ_1 and θ_2 and the longitudinal damage could not be contained, as illustrated by Figure 23 for the frames without crack stoppers, then the critical structural angle would be 40 degrees for the airplane illustrated. This already exceeds the 18 degree limit without considering any systems. The point here is that risk analysis does not eliminate the need to establish an onset of WFD which would degrade the residual strength capability below required levels in the event of discrete source damage.

A typical residual strength curve for the configuration without crack stopper straps is shown by the lower curve of Figure 19. The structural configuration here involved a fairly substantial frame section as shown by Figure 17. Figure 19 shows that the residual strength peak, given by point A, is above the typical applied principal stress for the discrete source damage case. If the frame member is of lighter construction, however, the peak A could be lower than the applied stress and the damage may not be arrested if fast fracture took place during the discrete source damage event. It may have been demonstrated during certification by harpoon testing that fast fracture would not take place. In fact this would be the case as illustrated by Figure 19. Suppose for example a 12 inch wide blade were used. Figure 19 shows that fast fracture would not occur even allowing for stable growth of say 2 inches making total damage length 14 inches. This would appear to satisfy the discrete source damage requirement. If on the other hand MSD had existed ahead of the lead damage as shown by Figure 27 link up would certainly occur extending the lead damage to a point where fast fracture would occur. If crack arrest capability at the outer frame does not exist, ie., point A of Figure 19 is below the applied principal stress, then explosive decompression would occur. The configuration shown by Figure 27 is particularly

difficult to deal with because crack tip bulging would be nearing a maximum as the tip approaches a point halfway between frames. For example, Table 2 shows for half crack length of 7.5 inches (total 15 inches) the values of β_S and β_B are 1.3779 and 1.526 respectively. β_S is higher than 1.0 because of the broken frame. Multiplying these values in equation 8 gives one of the most critical locations for link up as the crack moves across the bay. It appears that this condition is the most critical for those fuselages not able to contain a two bay crack with a broken frame.

FUSELAGE CIRCUMFERENTIAL CRACK

Probably one of the most critical locations for fuselage cracking is on the crown just over the rear spar of the wing at a location where circumferential frames are attached with shear clips. As indicated by Figure 14 the large damage criterion is to design for a two bay skin crack with a broken central stiffener for limit load. For most commercial transport aircraft the limit stress at this location is about 34 ksi. This damage scenario originates due to the fact that the stiffener, at the attachment to the frame, is critical in bending at the frame due to pressure. In addition, axial stresses are applied from fuselage down bending loads. The stiffener is critical in fatigue and if this cracks and fails and this condition remains undetected the skin becomes highly loaded and eventually cracks. The skin crack propagates into two bays. Figure 28 shows the residual strength curve for a typical location on the crown of the fuselage. The example shown assumes 2024-T3 skin 0.071 inches thick, hat section stiffeners with area 0.3029 square inches and stiffener spacing 8.0 inches. Stiffeners are 7075-T6 extrusions with ultimate tension strength 82 KSI. Skin fracture toughness is assumed 158 KSI $\sqrt{IN}$. The results of finite element analysis for this configuration are contained as case 15 of reference [14]. The residual strength calculation is shown in Table 7. The term R_{ct}, quoted in reference [14], is actually the reciprocal of β_S. The term σ_{os}, quoted in Table 7, is the stress concentration factor in the stiffener, ie., the stiffener outer fiber stress per KSI of applied gross stress. The residual strength for the two bay crack condition is given by the intersection of the skin fracture and outer stiffener strength curves at point A. Any fast fracture at a gross stress lower than this point would be arrested. Fast fracture at stresses higher than point A would not be arrested and failure would be precipitated by stiffener strength criteria. It can be seen that this configuration is able to tolerate a two bay skin crack at the limit stress of 34 KSI. The effect of MSD is shown and illustrates the considerable loss in residual strength to well below limit capability. The calculations for the 0.05 inch MSD crack configuration, based on equation 5, are shown in Table 8. The calculations for the 0.01 inch MSD crack are similar. Rivet spacing in the circumferential direction is assumed to be 1.0 inches. As mentioned earlier the effect due to a very small crack such as 0.01 inches appears quite severe. One needs to remember that this crack is at both sides of a fastener hole and therefore it is effectively a crack of length 2(0.01) + rivet diameter. This is one area which would need a fairly detailed

investigation to find MSD small enough so as not to degrade the residual strength capability below limit strength.

ONSET OF MSD

Several examples of the effect of MSD in lead crack residual strength have been shown in this paper. It is evident that this analysis, based on the intuitive link up criterion illustrated by Figure 9, indicates considerable effects of structural configuration. The gross applied stress at link up appears to be more sensitive to rivet spacing than the size of MSD once it is assumed that a crack exists in the hole at the tip of the lead crack. Some configurations are able to tolerate much larger MSD sizes than other configurations. This was illustrated by the improvement in capability provided by a configuration with titanium crack stopper straps for the discrete source damage case. Each susceptible area needs to be assessed for the size of MSD which will degrade the lead crack residual strength below limit load. The time in the life of the aircraft at which this occurs will then need to be estimated. One way to obtain this is by a crack growth analysis starting with flaw sizes representative of the initial quality of the structure. This method is described in reference [18] which describes a test program designed to develop equivalent initial flaw sizes for various hole and fastener combinations. Figure 29 shows a typical example of equivalent initial flaw size plotted against cumulative probability. This data, reported in reference[2], was statistically analyzed to obtain a 95% confidence level. The example on Figure 29 shows that it can be assured with 95% confidence that 90% of the flaws would be less than 0.0012 inches. The example shown is for open reamed countersunk holes. Filled holes would most likely indicate a smaller size. This size falls into the well known "short crack problem" area so care would need to be exercised in growth calculations which use large crack da/dN data. Crack growth data would need to be generated at small crack sizes. Some people believe that short crack growth can be accurately calculated using Forman's equation which does not reflect a threshold value. This author has had some success with this as can be seen by Figure 21 of reference [18]. In this case growth rate was simulated by a Forman equation and crack growth started at 0.001 inches. The loading used was for a STOL transport aircraft spectrum and the Generalized Willenborg retardation model was used. Crack size was measured by striation count using an electron microscope on the failed fracture surface.

It is suggested that statistically determined equivalent initial quality flaw data could be used without any additional factors. The reliability would already be included with the flaw size chosen to represent a specific reliability and confidence level. This method would establish a life associated with a specific reliability level providing the time at which the lead damage residual strength level would be degraded below the regulatory level for the specific structural configuration being considered. Obviously, those designs with greater resistance to residual strength loss due to MSD would

provide longer onset times. Further discussion of the Equivalent Initial Quality Flaw concept can be found in a paper by Dr. John W. Lincoln [19].

The proposed monitoring period defined in Figure 1 could probably be reliably used to verify MSD onset prior to residual strength loss in the case where titanium crack stopper straps form a part of the design. However, where the design does not include crack stoppers considerable difficulty would be experienced finding the MSD before residual strength dropped below the required levels.

EFFECT OF EXTERNAL REPAIRS

Figure 30 illustrates a potential problem created by external repair doublers. Many of these repairs to fuselage skins are designed to meet static strength requirements only and virtually no consideration is given to damage tolerance capability. Many of these repairs are too thick causing high load transfer at the first row of fasteners. There is a possibility that hidden MSD in the skin under the doubler may lead to loss in lead crack residual strength as indicated in Figure 30. This problem is discussed in more detail in reference [20].

CONCLUSIONS

1) It has been shown using an intuitive link up criterion that MSD can have considerable effect on lead crack residual strength in complex stiffened structures.

2) The loss in residual strength is extremely sensitive to structural configuration and fastener spacing.

3) Frames with crack stoppers in fuselage structure provide much greater tolerance to MSD than frames without crack stoppers.

4) The industry proposed monitoring period to verify the onset of MSD may be reliable for some structural configurations and unreliable for others.

5) In-service inspection techniques will not be adequate for some structural configurations to validate the onset of WFD established by the manufacturers prior to loss in residual strength below limit.

6) Validation of the onset of WFD during the monitoring period may require local tear down inspection in order to find MSD before certified residual strength is degraded for some structural configurations.

RECOMMENDATIONS

1) It is recommended the FAA continue support for testing required to validate lead crack/MSD link up for complex stiffened structure.

2) It is recommended that the "Equivalent Initial Quality Flaw" concept be investigated to assist in establishing onset of WFD. Further research is needed to improve the reliability of prediction methods to grow short cracks of the order of 0.001 inches up to a size which would cause lead crack residual strength to be degraded below limit values.

3) Recommendation 2 may need further research on crack growth rate da/dN data for short cracks in materials used in the commercial aircraft industry.

4) It is recommended that research for MSD be concentrated on the effects of MSD on lead crack residual strength rather than on crack growth investigations with a view to establishing inspection programs to manage the safety of aircraft in the presence of MSD.

REFERENCES

[1] Air Transportation Association of America Final Report. Airworthiness Assurance Task Force Subcommittee on Fatigue Testing and/or Teardown Issues. February 1991.

[2] Swift, T., "Verification of Methods For Damage Tolerance Evaluation of Aircraft Structures to FAA Requirements". Presented at the 12th Symposium of the International Committee on Aeronautical Fatigue held in Toulouse, France, May 1983.

[3] Swift, T., "The Influence of Slow Growth and Net Section Yielding on the Residual Strength of Stiffened Structure". Presented at the 13th Symposium of the International Committee on Aeronautical Fatigue held in Pisa, Italy, May 1985.

[4] Swift, T., "Damage Tolerance in Pressurized Fuselages". 11th Plantema Memorial Lecture. Presented at the 14th Symposium of the International Committee on Aeronautical Fatigue held in Ottawa, Canada, June 1987.

[5] Swift, T., "Damage Tolerance Capability". Presented at Specialist' Conference on Fatigue of Aircraft Materials. Delft University of Technology, Delft, The Netherlands, October 1992.

[6] Liu, A.F., "Statistical Variation in Fracture Toughness Data of Airframe Materials". Published in Proceedings of the Air Force Conference on Fatigue and Fracture of Aircraft Structures and Materials. AFFDL TR 70-144. September 1970.

[7] Wang, D.Y., "Plane Stress Fracture Toughness and Fatigue Crack Propagation of Aluminum Alloy Wide Panels". Presented to Sixth National Symposium on Fracture Mechanics, ASTM. Philadelphia, Pennsylvania, August 1972.

[8] Feddersen, C.E. "Evaluation and Prediction of the Residual Strength of Center Cracked Tension Panels". Published in "Damage Tolerance in Aircraft Structures ASTM STP 486, 1971.

[9] Private Communication with Dr. Ron Mayville of A.D. Little Inc.

[10] Rooke, D.P. and Cartwright, D.J., "Compendium of Stress Intensity Factors". Published by Her Majesty's Stationary Office, London, England, 1976.

[11] Broek, D., "Elementary Engineering Fracture Mechanics". Published by Martinus Nijhoff Publishers, 1974.

[12] Private Communication : Commander Jim Moukawsher, USCG, Dec. 1992.

[13] Bowie, O.L., "Analysis of an Infinite Plate Containing Radial Cracks Originating from the Boundary of an Internal Circular Hole," Journal of Mathematics and Physics, Vol. 35, 1956.
[14] Swift, T., "Development of the Fail-Safe Design Features of the DC-10. Published in "Damage Tolerance in Aircraft Structures". ASTM STP 486, 1971.

[15] Swift, T and Wang, D.Y., "Damage Tolerant Design-Analysis Methods and Test Verification of Fuselage Structure". Published in Proceedings of the Air Force Conference on Fatigue and Fracture of Aircraft Structures and Materials. AFFDL TR 70-144, September 1970.

[16] Kuhn, P., "Notch Effects on Fatigue and Static Strength". Published in Proceedings of ICAF Symposium held in Rome, 1963.

[17] Private Communication with Prof. Dr. Lüder Schwarmann dated 3 June, 1991.

[18] Stone, M and Swift, T., "Future Damage Tolerance Approach to Airworthiness Certification". Presented at the 10th Symposium of the International Committee on Aeronautical Fatigue held in Brussels, Belgium, May 1979.

[19] Lincoln, J.W., "Assessment of Structural Reliability Derived From Durability Testing". Presented at the 17th Symposium of the International Committee on Aeronautical Fatigue held in Stockholm, Sweden, June 1993.

[20] Swift, T., "Repairs to Damage Tolerant Aircraft". Presented at The International Symposium on Structural Integrity of Aging Airplanes. Atlanta, Georgia, March 1990. FAA-AIR-90-01.

Table 1
Residual Strength Calculation
Two Bay Longitudinal Crack - Frames With Crack Stoppers - Center Frame and Crack Stopper Failed

(1)	(2)	(3)	(4)	(5)
a	β_S	β_B	$\beta_S\beta_B[\pi a]^{1/2}$	σ_R
4.50	1.2870	1.3560	6.5617	24.08
7.50	1.2136	1.5260	8.9895	17.58
10.50	1.1534	1.6020	10.6124	14.89
12.75	1.1161	1.5800	11.1607	14.16
15.50	1.0482	1.4530	10.6280	14.87
17.50	0.9681	1.2880	9.2455	17.09
18.50	0.8993	1.1840	8.1174	19.46
19.50	0.7133	1.0646	5.9436	26.58
20.50	0.5155	1.0646	4.4042	35.87
21.50	0.5200	1.1840	5.0600	31.23

Material 0.071 2024-T3 K_c Assumed 158 KSI $[IN]^{1/2}$

$\sigma_R = 158/(4)$

Table 2
Residual Strength Calculation
Two Bay Longitudinal Crack - Frames Without Crack Stoppers - Center Frame Failed

a	β_S	β_B	$\beta_S\beta_B[\pi a]^{1/2}$	σ_R
4.50	1.4741	1.3560	7.5157	21.02
7.50	1.3779	1.5260	10.2065	15.48
10.50	1.3160	1.6020	12.1084	13.05
12.75	1.2707	1.5800	12.7066	13.09
15.50	1.1962	1.4530	12.1268	13.03
17.50	1.1139	1.2880	10.6379	14.85
18.50	1.0541	1.1840	9.5147	16.61
19.50	0.9589	1.0646	7.9901	19.77
20.50	0.8565	1.0646	7.3212	21.58
21.50	0.8005	1.1840	7.7895	20.28

Material 0.071 2024-T3 K_c Assumed 158 KSI $[IN]^{1/2}$

$\sigma_R = 158/(4)$

Table 3
Effect of 0.05 Inch MSD on Residual Strength
Two Bay Longitudinal Crack - Frames With Crack Stoppers -
Center Frame and Crack Stopper Failed

a_2	β_S	β_B	a_{e2}	a_{e2}/b	β_{I1}	β_{I2}	σ_R
19.5	0.7133	1.0646	11.24	9.73	2.44	1.0	20.34
20.5	0.5155	1.0646	6.17	5.34	2.01	1.0	27.19
21.5	0.5200	1.1840	8.15	7.06	2.12	1.0	23.85

$a_{e2} = (\beta_S\beta_B)^2 a_2$, $a_1 = \beta_h^2 a_1 = 1.057^2(0.145) = 0.162$ (constant)

$b = 1.25-0.095 = 1.155$, $a_{e1}/b = 0.162/1.55 = 0.1403$

$$\sigma_R = \{2\sigma_y^2(P-d/2-a_1)/[\beta_h^2\beta_{I1}^2 a_1 + (\beta_S\beta_B)^2\beta_{I2}^2 a_2]\}^{1/2}$$

$$\sigma_R = \{5050/[0.162\beta_{I1}^2 + (\beta_S\beta_B)^2\beta_{I2}^2 a_2]\}^{1/2}$$

Table 4
Effect of 0.05 Inch MSD on Residual Strength
Two Bay Longitudinal Crack - Frames without Crack Stoppers -
Center Frame Failed

a_2	β_S	β_B	a_{e2}	a_{e2}/b	β_{I1}	β_{I2}	σ_R
19.5	0.9589	1.0646	20.32	17.59	3.31	1.0	15.12
20.5	0.8565	1.0646	17.04	14.75	3.01	1.0	16.52
21.5	0.8005	1.1840	19.31	16.72	3.22	1.0	15.50

Reference Table 8 for a_{e2}, a_{e1}, b, a_{e1}/b and σ_R

Table 5
Effect of 0.05 Inch MSD on Residual Strength
Two Bay Longitudinal Crack - Frames With Crack Stoppers -
Rivet Spacing 1.0 Inches

a_2	β_S	β_B	a_{e2}	a_{e2}/b	β_{I1}	β_{I2}	σ_R
19.5	0.7133	1.0646	11.24	12.420	2.80	1.0	17.43
20.5	0.5155	1.0646	6.17	6.820	2.11	1.0	23.48
21.5	0.5200	1.1840	8.15	9.006	2.38	1.0	20.47

$a_{e2} = (\beta_S\beta_B)^2 a2$, $a_{e1} = \beta_h^2 a_1 = 1.057^2(0.145) = 0.162$ (constant)
$b = 1.0 - 0.095 = 0.905$, $a_{e1}/b = 0.162/0.905 = 0.179$
σ_R based on equation 8 with $\sigma_y = 50$ KSI

Table 6

Effect of 0.05 Inch MSD on Residual Strength
Two Bay Longitudinal Crack - Frames Without Crack Stoppers -
Rivet Spacing 1.0 Inches

a_2	β_S	β_B	a_{e2}	a_{e2}/b	β_{I1}	β_{I2}	σ_R
19.5	0.9589	1.0646	20.32	22.45	3.84	1.0	12.94
20.5	0.8565	1.0646	17.04	18.83	3.50	1.0	14.13
21.5	0.8005	1.1840	19.31	21.34	3.76	1.0	13.26

Table 7
Results of Typical Finite Element Analysis
For Circumferential Crack

(1)	(2)	(3)	(4)	(5)	(6)
a	R_{ct}	β_s	σ_r	σ_{os}	σ_{st}
1.5	0.778	1.285	56.64	1.074	76.35
2.5	0.820	1.220	46.21	1.114	73.61
3.5	0.852	1.174	40.59	1.176	69.73
4.5	0.883	1.133	37.09	1.269	64.62
5.5	0.918	1.089	34.90	1.414	57.99
6.5	0.970	1.031	33.91	1.660	49.40
7.5	1.107	0.903	36.05	2.153	38.09
8.5	1.353	0.739	41.37	3.212	25.53
9.5	1.428	0.700	41.32	3.875	21.16

(3) = 1/(2)
(4) = $158/[(\pi a)^{1/2}\beta_s]$
(6) = 82/(5)

K_c = 158 KSI $[IN]^{1/2}$

F_{tu} = 82 KSI

Table 8
Effect of 0.05 inch MSD Crack on Lead Crack Residual Strength
Two Bay Circumferential Crack With Broken Central Stiffener

a_2	β_s	a_{e2}	a_{e1}/b *	a_{e2}/b **	β_{I1}	β_{I2}	σ_R
1.5	1.285	2.477	0.179	2.737	1.50	1.0	36.57
2.5	1.220	3.721	0.179	4.112	1.75	1.0	30.02
3.5	1.174	4.824	0.179	5.330	1.92	1.0	26.48
4.5	1.133	5.777	0.179	6.383	2.05	1.0	24.26
5.5	1.089	6.523	0.179	7.208	2.16	1.0	22.85
6.5	1.031	6.909	0.179	7.634	2.20	1.0	22.22
7.5	0.903	6.116	0.179	6.758	2.10	1.0	23.59
8.5	0.739	4.642	0.179	5.129	1.92	1.0	26.93
9.5	0.700	4.655	0.179	5.144	1.92	1.0	26.90

* 0.162/0.905, ** $a_{e2}/0.905$, $a_{e2} = \beta_s^2 a_2$

$$\sigma_R = \{2\sigma_y^2(P-d/2-a_1)/(\beta_h^2\beta_{I1}^2 a_1 + \beta_s^2\beta_{I2}^2 a_2)\}^{1/2}$$

$$\sigma_R = \{3800/(0.162\beta_{I1}^2 + \beta_s^2\beta_{I2}^2 a_2)\}^{1/2}$$

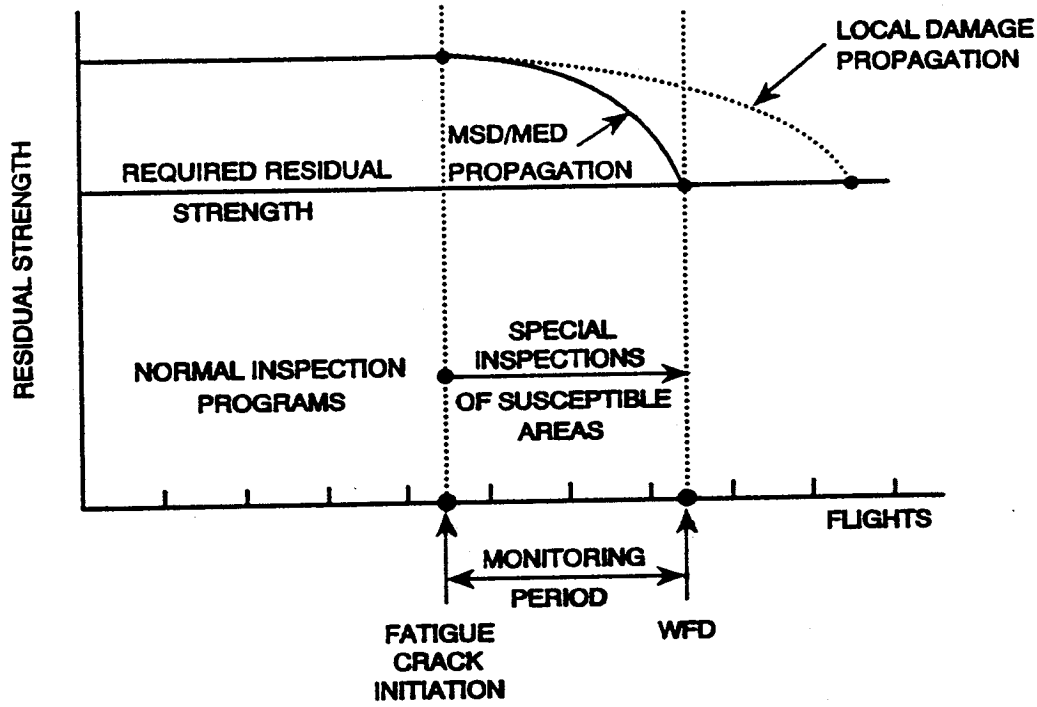

FIGURE 1 RESIDUAL STRENGTH CAPABILITY AND RESULTING INSPECTION ACTIONS

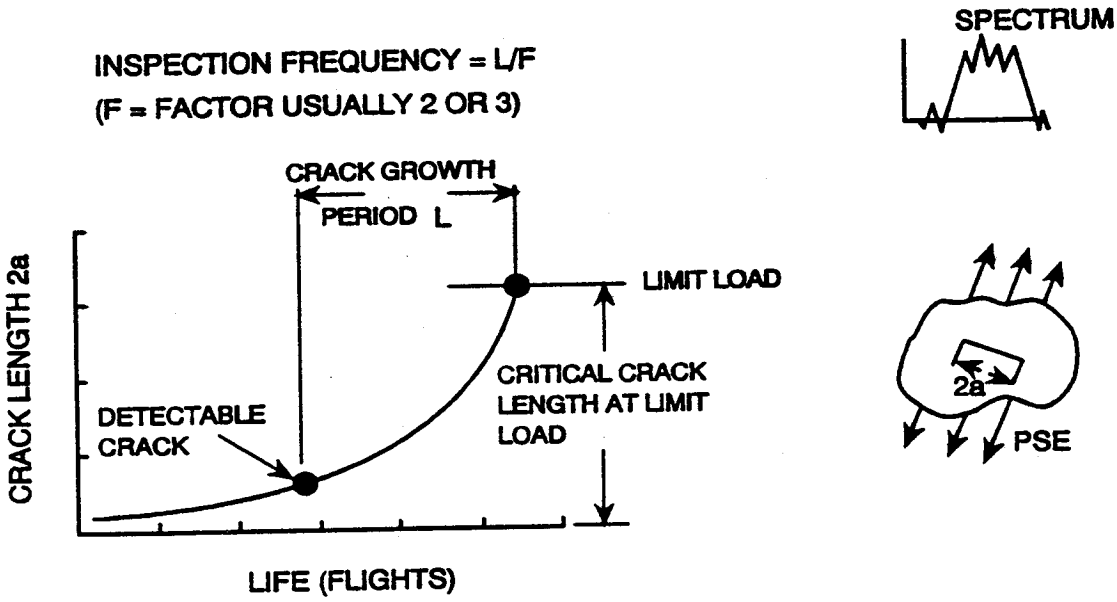

FIGURE 2 INSPECTION FREQUENCY FOR EACH PSE IS RELATED TO CRITICAL CRACK LENGTH

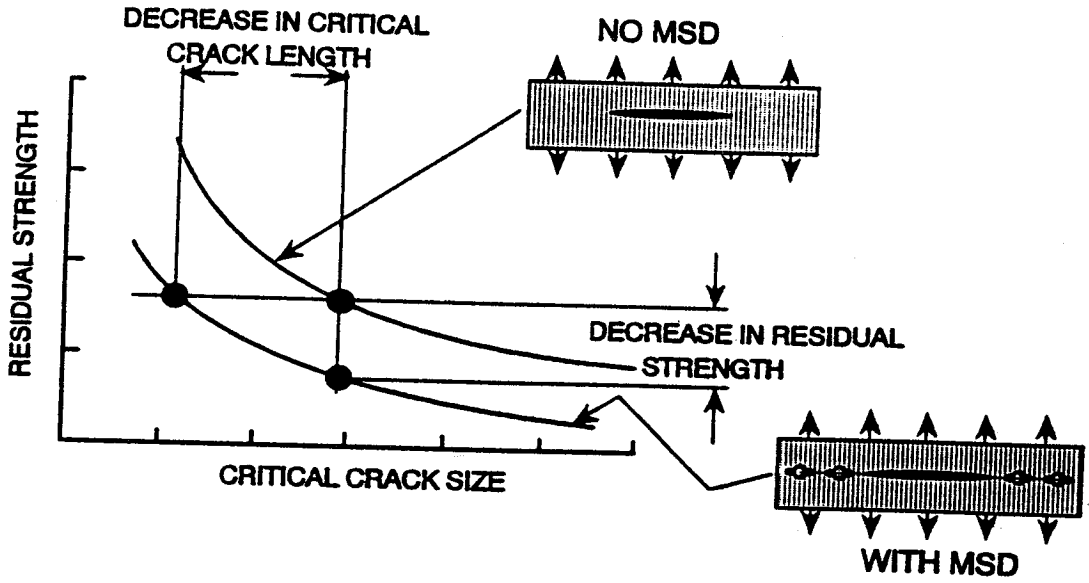

FIGURE 3 EFFECT OF MSD ON CRITICAL CRACK SIZE AND RESIDUAL STRENGTH

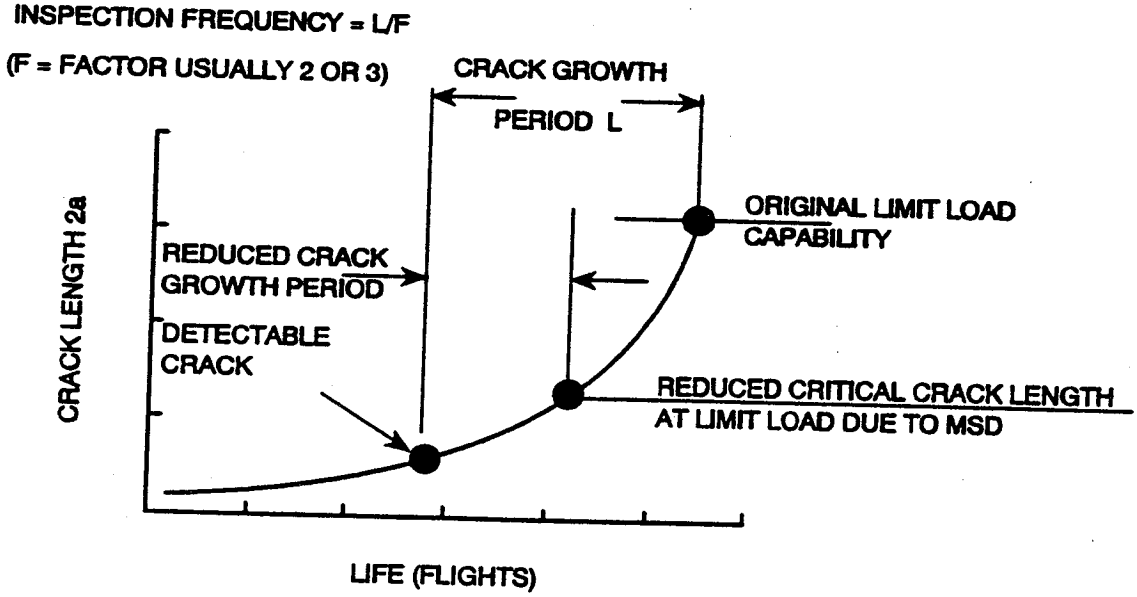

FIGURE 4 REDUCED LEAD CRACK INSPECTION FREQUENCY RESULTING FROM REDUCED CRITICAL CRACK SIZE DUE TO MSD

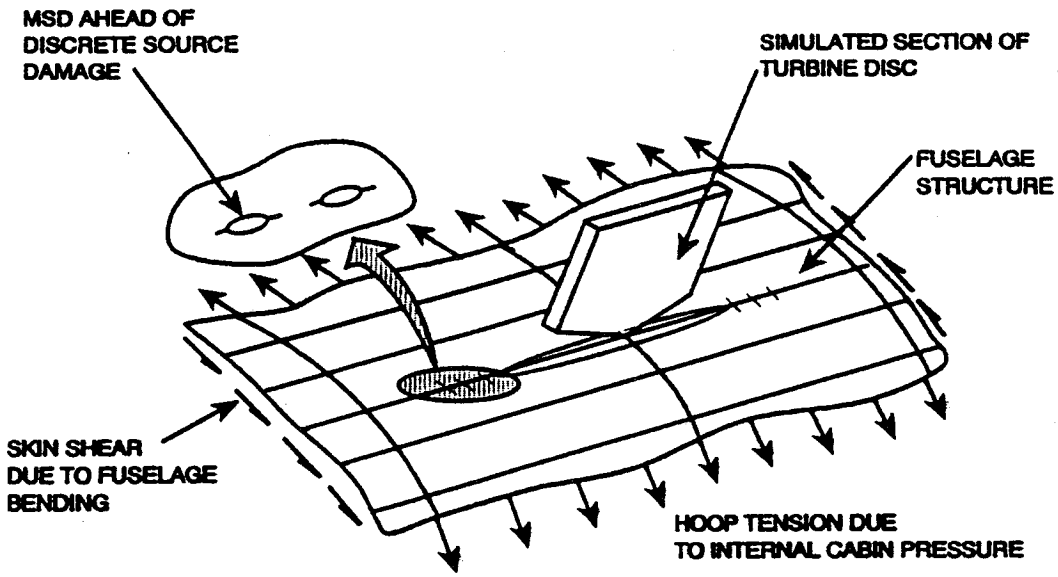

FIGURE 5 EFFECT OF MSD ON RESIDUAL STRENGTH CAPABILITY DUE TO DISCRETE SOURCE DAMAGE

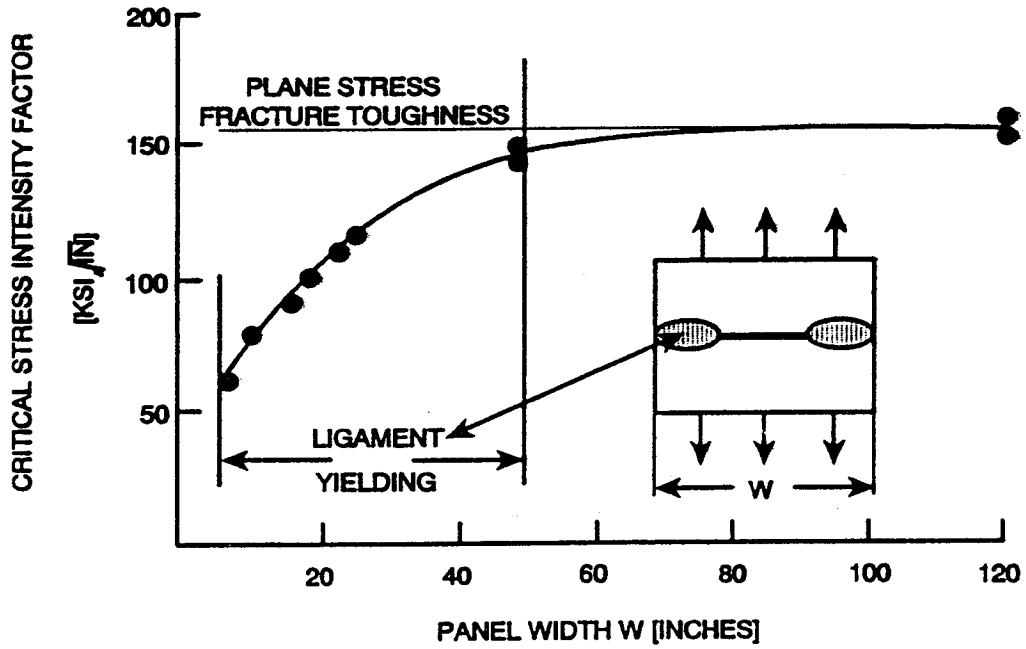

FIGURE 6 CRITICAL STRESS INTENSITY FACTOR VERSUS PANEL WIDTH FOR LEAD CRACKS IN 2024-T3 SHEET 0.063 INCHES THICK

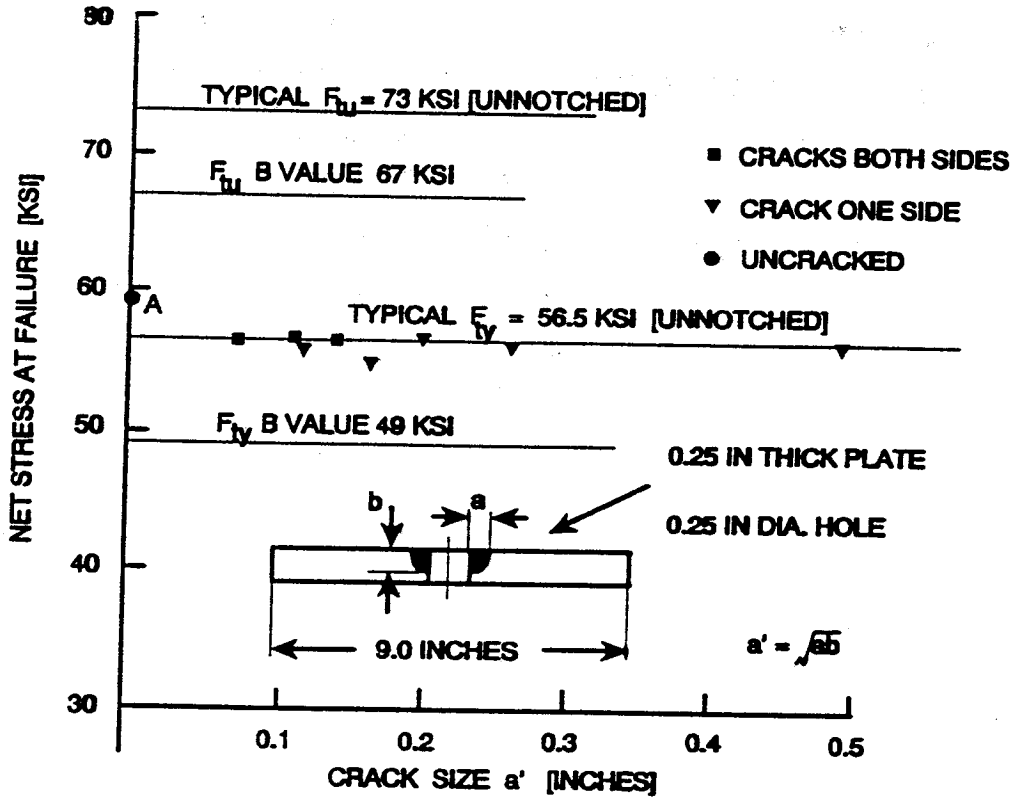

FIGURE 7 RESIDUAL STRENGTH FOR SMALL CRACKS IN 2024-T351 PLATE

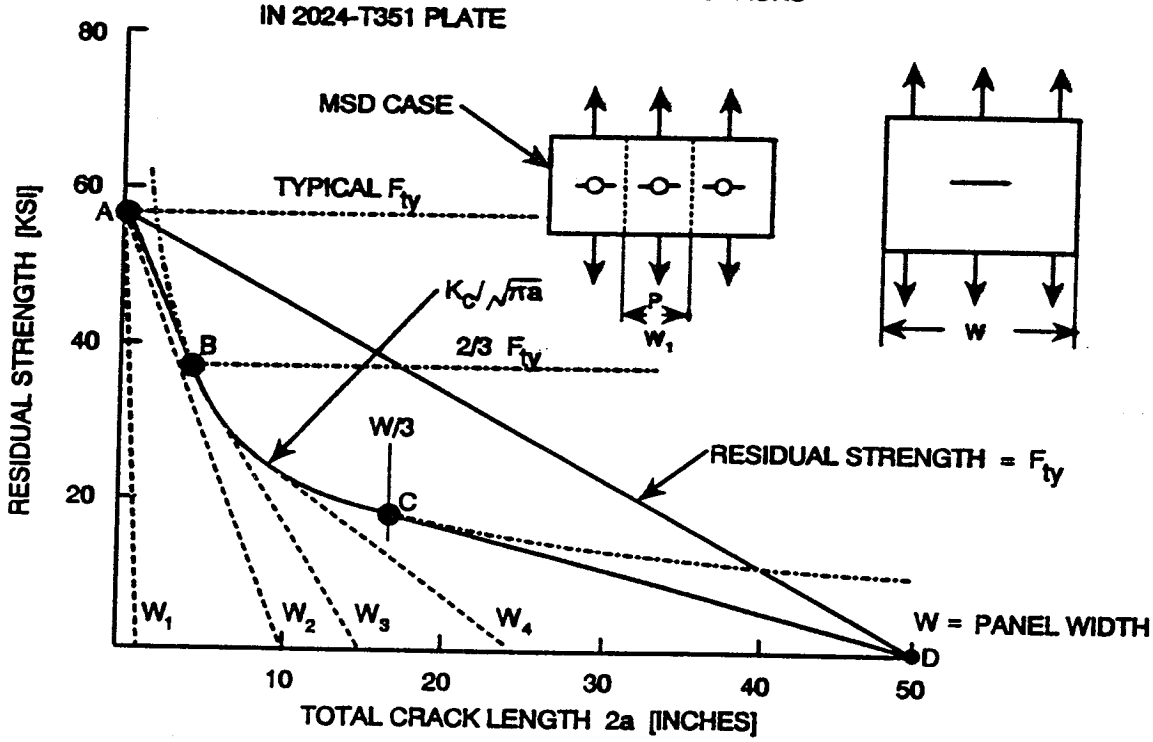

FIGURE 8 TYPICAL UNSTIFFENED PANEL RESIDUAL STRENGTH DIAGRAM BASED ON FEDDERSEN'S METHOD 2024-T351 PLATE

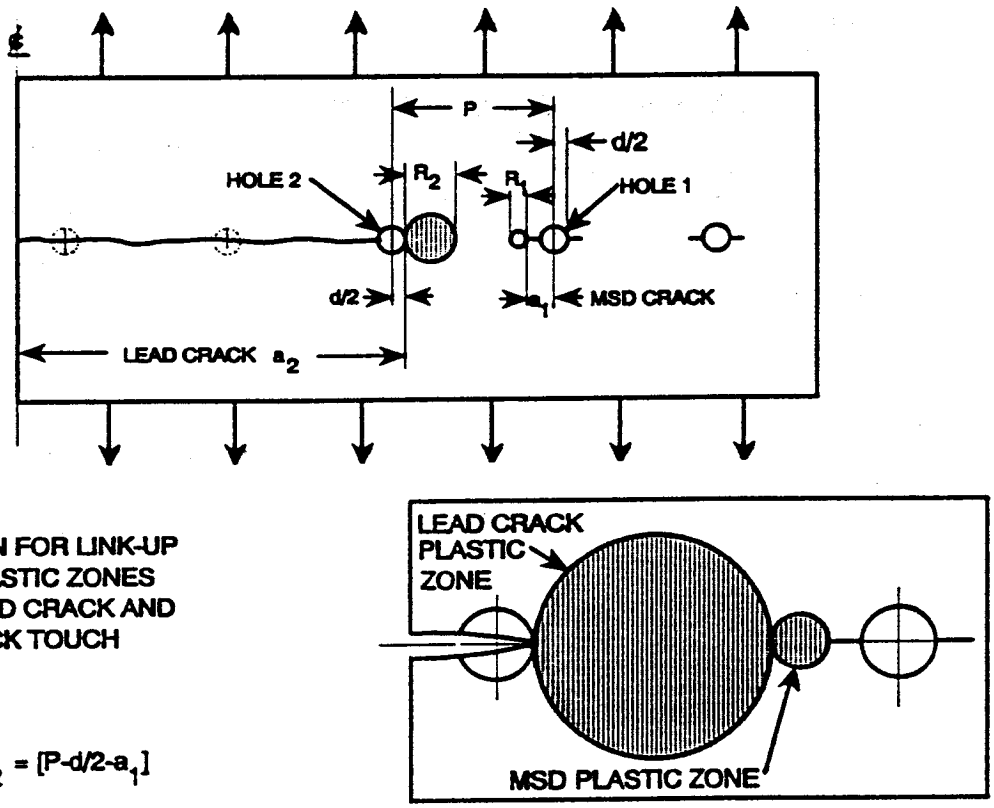

FIGURE 9 LEAD CRACK - MSD CRACK LINK-UP CRITERION

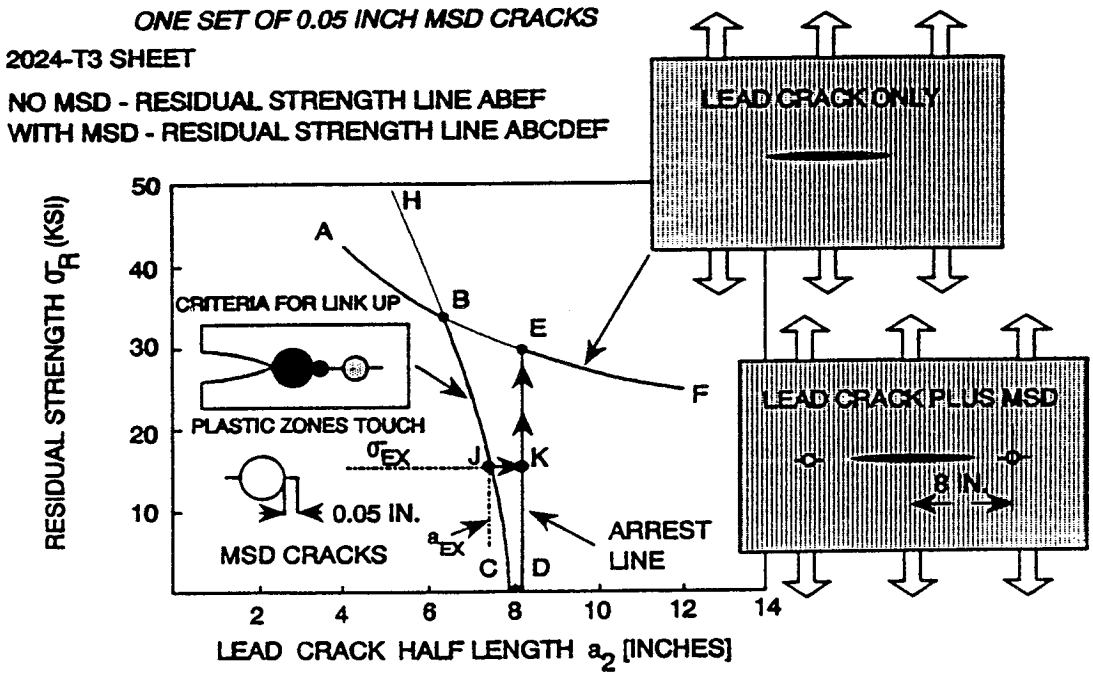

FIGURE 10 EFFECT OF MSD ON LEAD CRACK RESIDUAL STRENGTH
SINGLE 0.05 INCH MSD CRACK EACH SIDE OF LEAD CRACK

TWO SETS OF 0.05 IN.MSD CRACKS

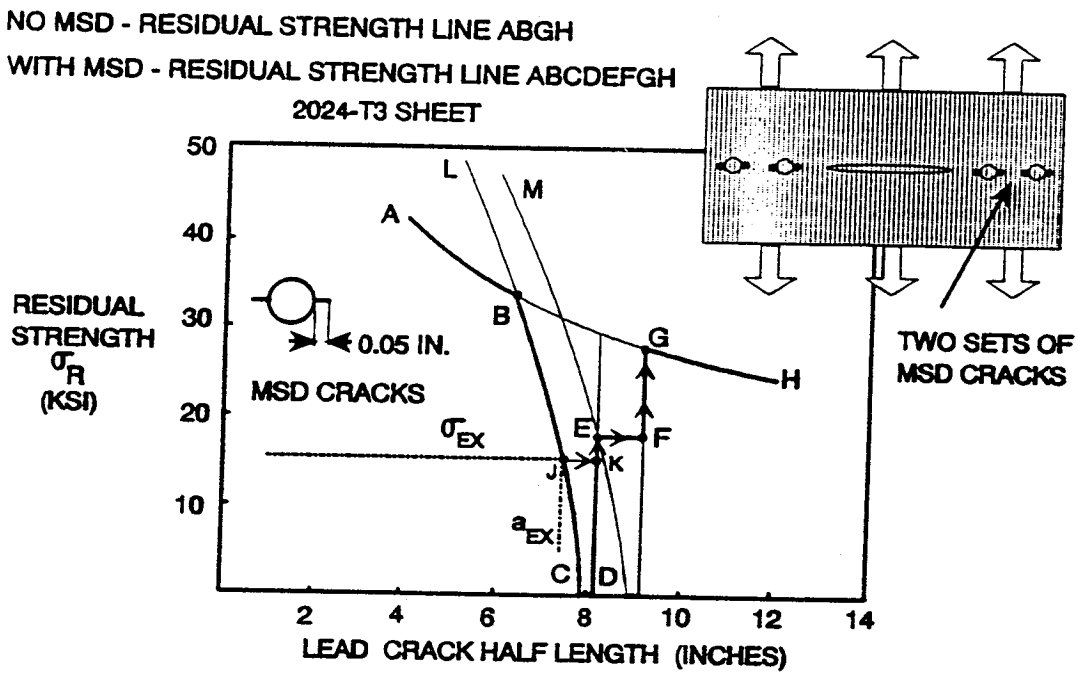

FIGURE 11 EFFECT OF MSD ON LEAD CRACK RESIDUAL STRENGTH
TWO SETS OF 0.05 INCH MSD CRACKS EACH SIDE OF LEAD CRACK

SEVERAL 0.05 IN. MSD CRACKS

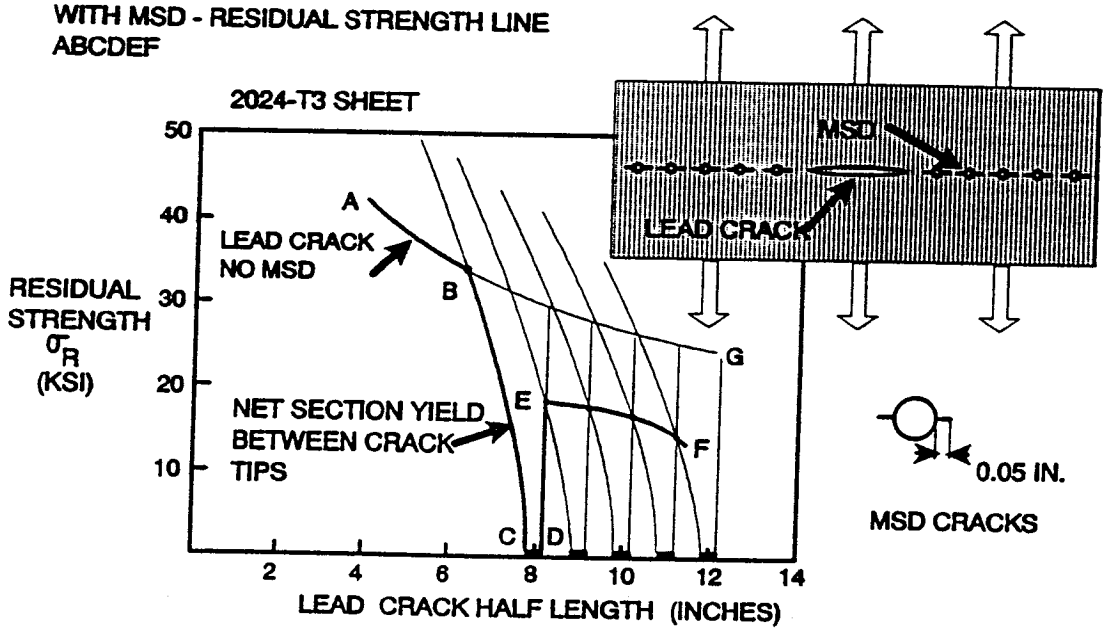

FIGURE 12 EFFECT OF MSD ON LEAD CRACK RESIDUAL STRENGTH
SEVERAL 0.05 INCH MSD CRACKS EACH SIDE OF LEAD CRACK

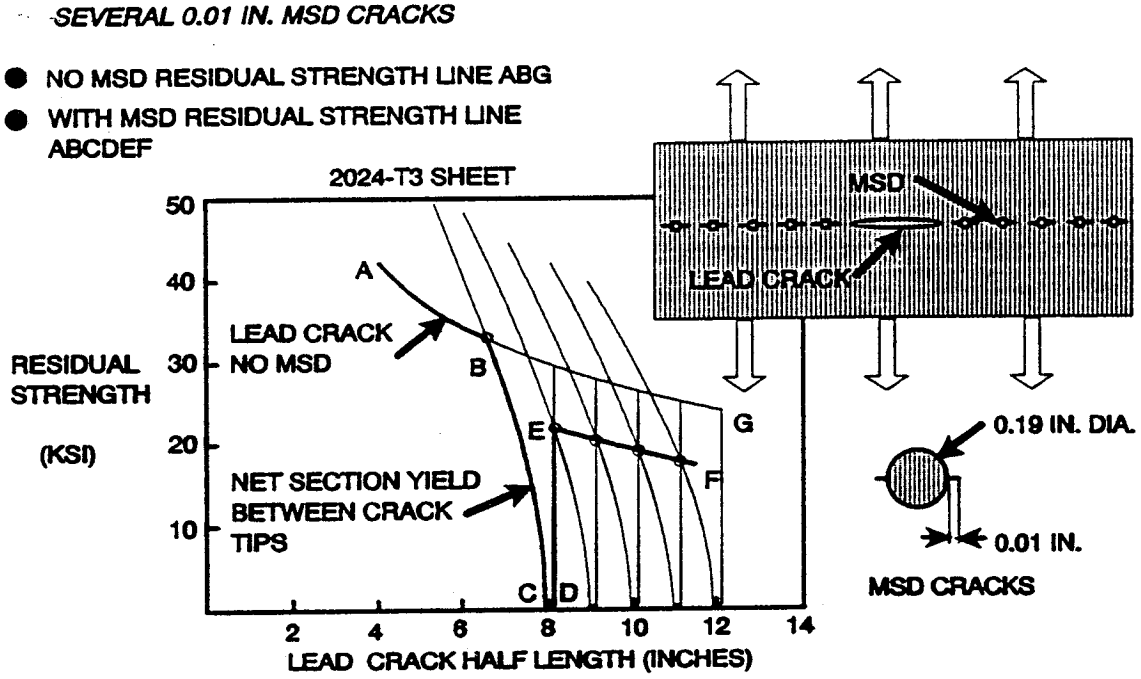

FIGURE 13 EFFECT OF MSD ON LEAD CRACK RESIDUAL STRENGTH
SEVERAL 0.01 INCH CRACKS EACH SIDE OF LEAD CRACK

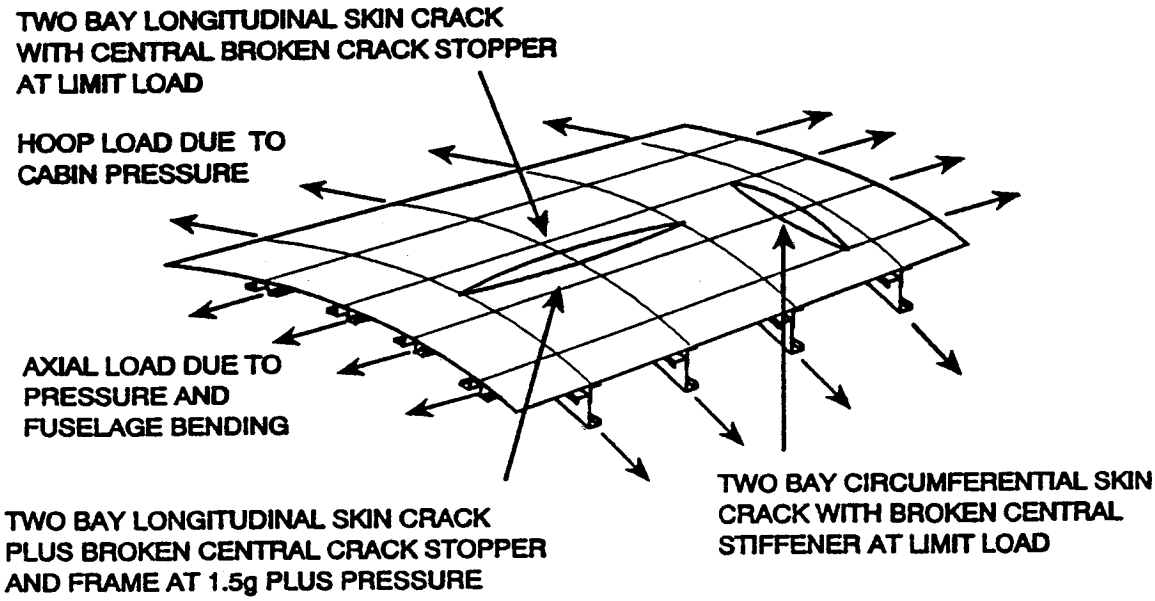

FIGURE 14 FUSELAGE DAMAGE SIZES USED FOR LARGE DAMAGE SUBSTANTIATION

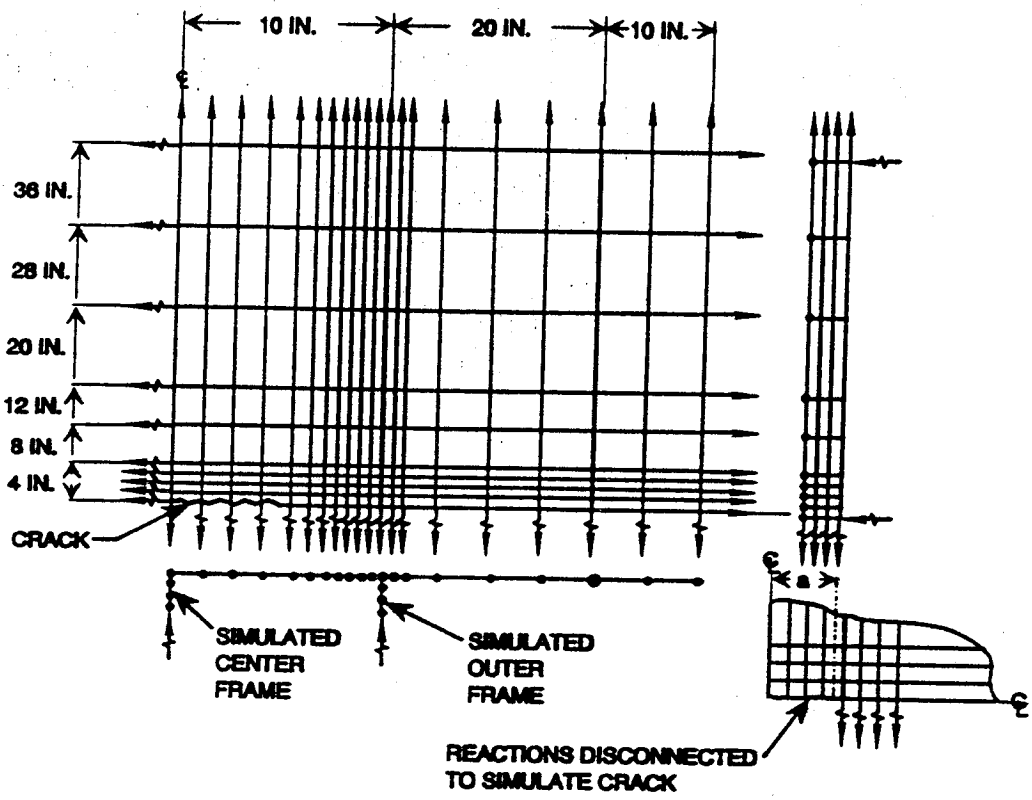

FIGURE 15 IDEALIZATION FOR TWO BAY LONGITUDINAL CRACK

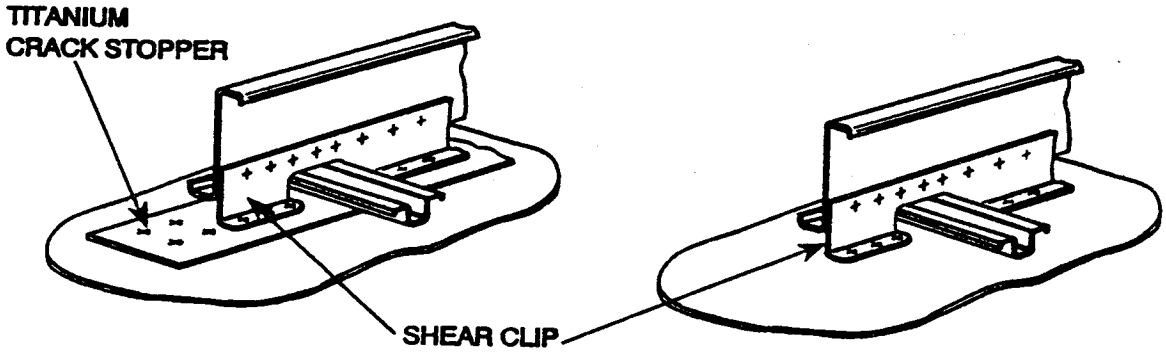

FIGURE 16 TWO TYPES OF CIRCUMFERENTIAL FRAME DESIGNS IN COMMERCIAL TRANSPORT AIRCRAFT

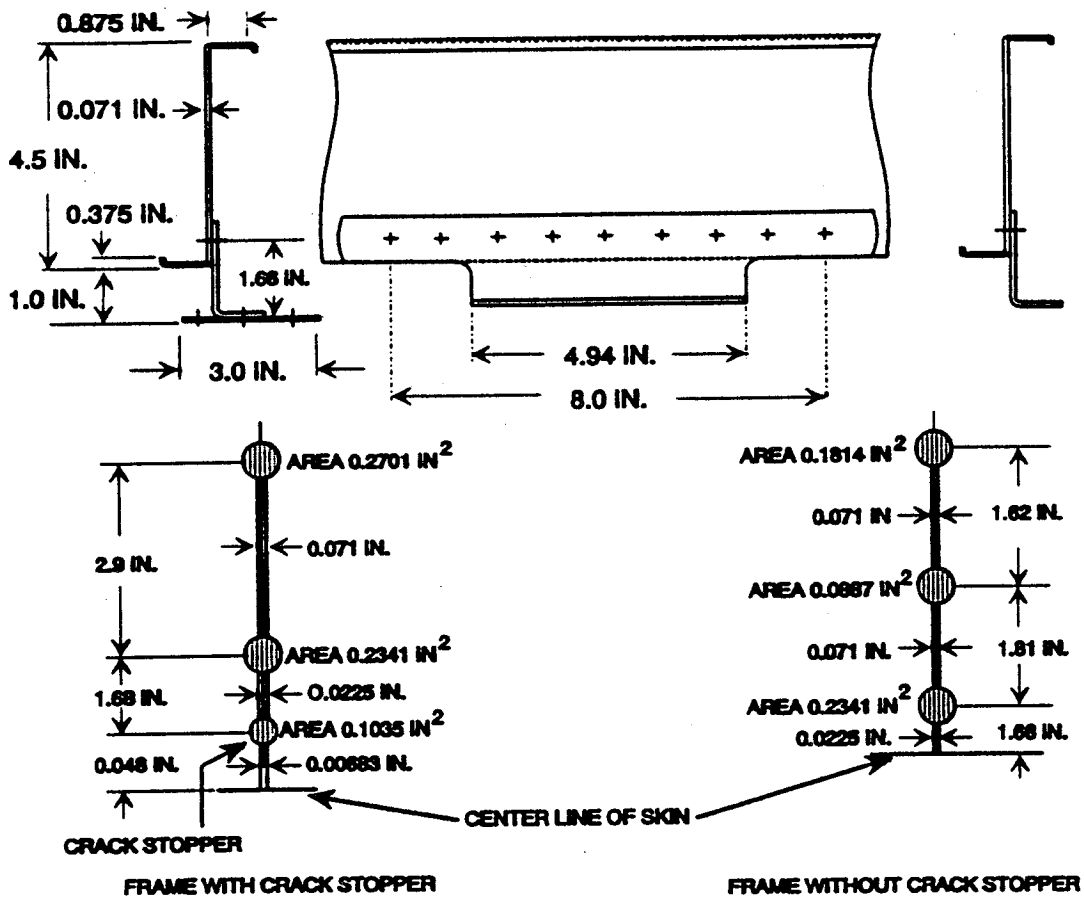

FIGURE 17 CIRCUMFERENTIAL FRAME IDEALIZATION

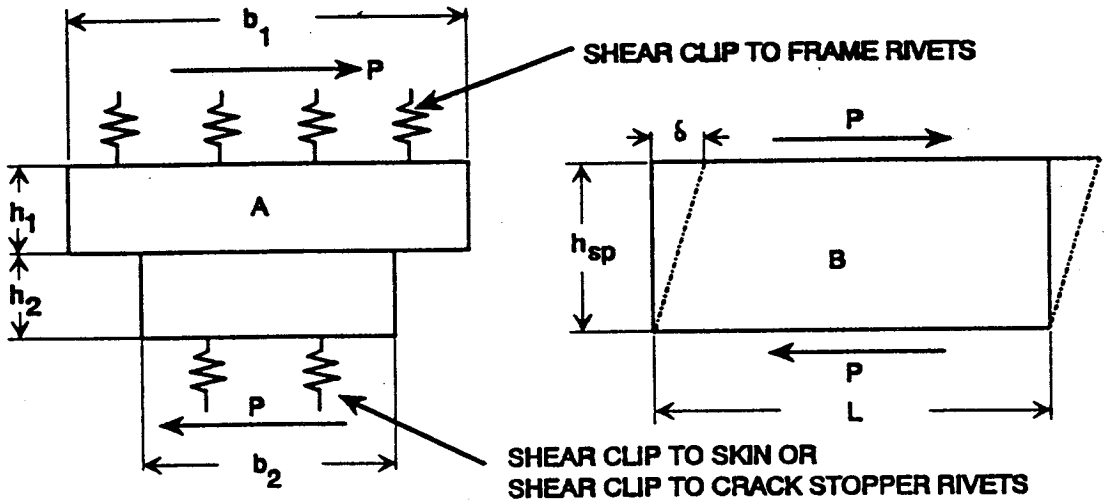

FIGURE 18 SHEAR CLIP IDEALIZATION

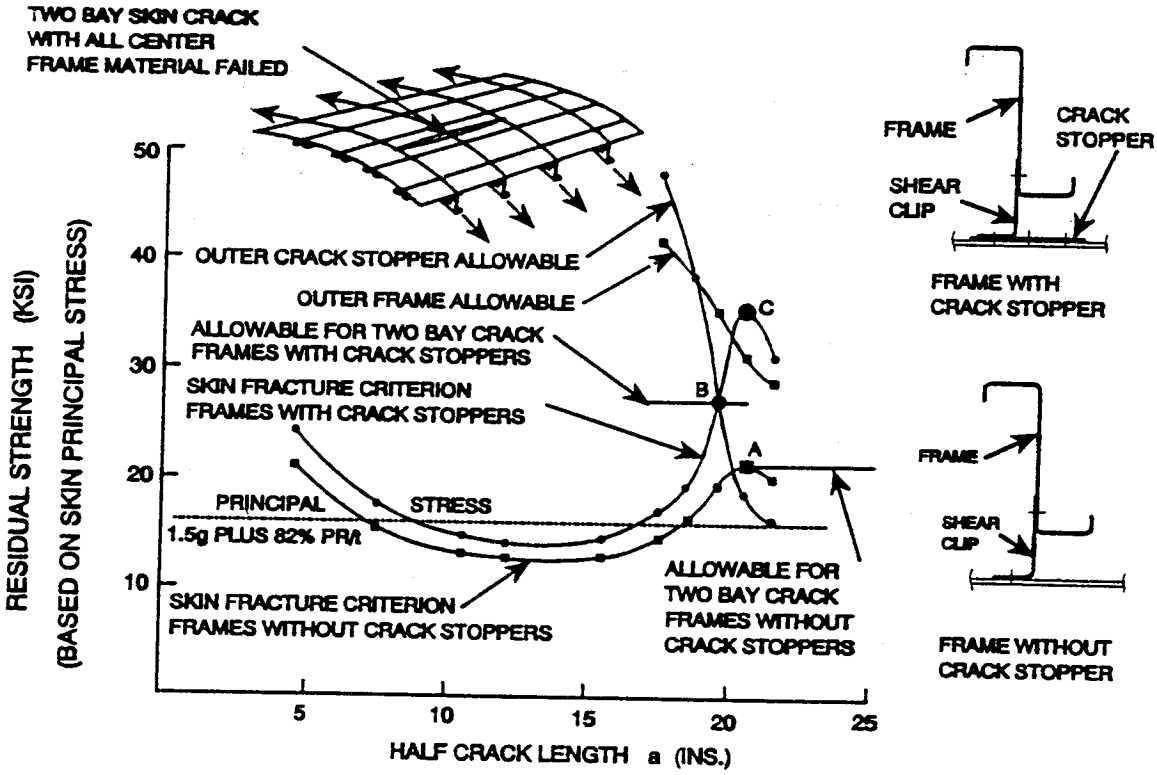

FIGURE 19 RESIDUAL STRENGTH COMPARISON
FRAMES WITH AND WITHOUT CRACK STOPPERS

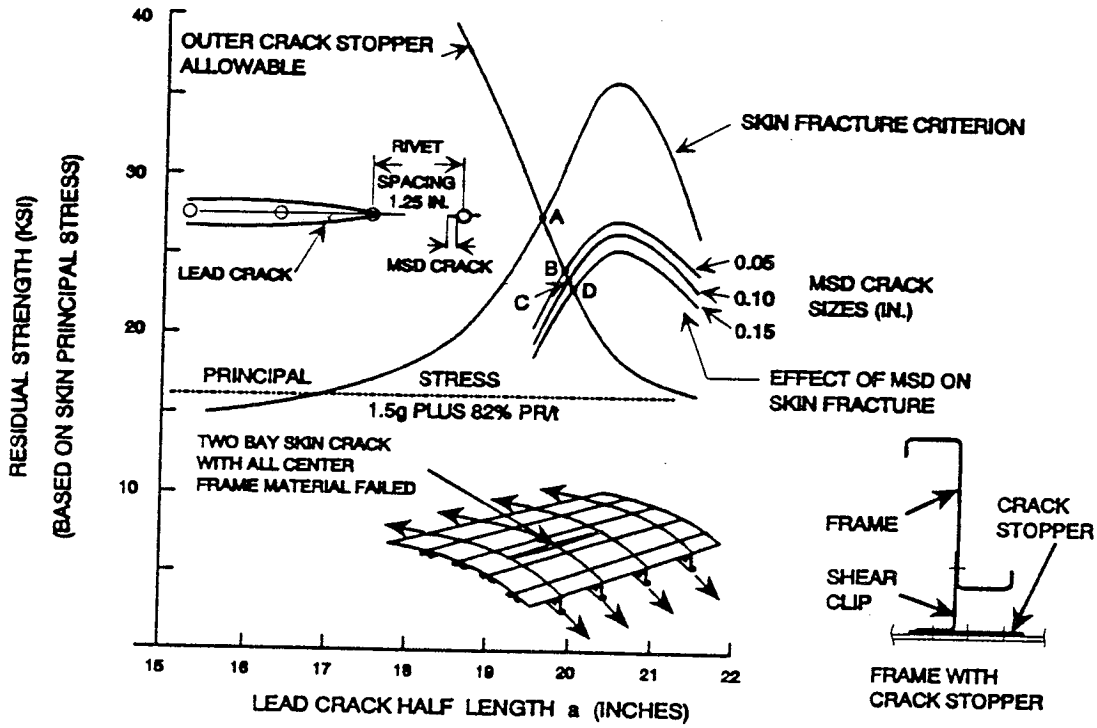

FIGURE 20 EFFECT OF MSD ON LEAD CRACK RESIDUAL STRENGTH
FRAMES WITH CRACK STOPPERS - RIVET SPACING 1.25 IN.

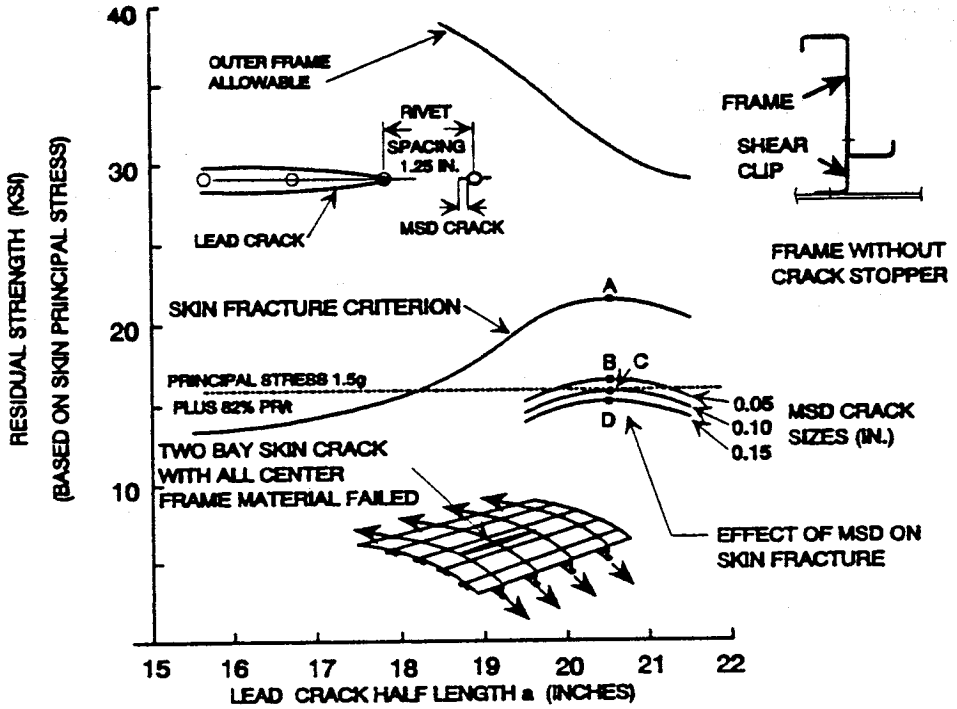

FIGURE 21 EFFECT OF MSD ON LEAD CRACK RESIDUAL STRENGTH
FRAMES WITHOUT CRACK STOPPERS - RIVET SPACING 1.25 IN.

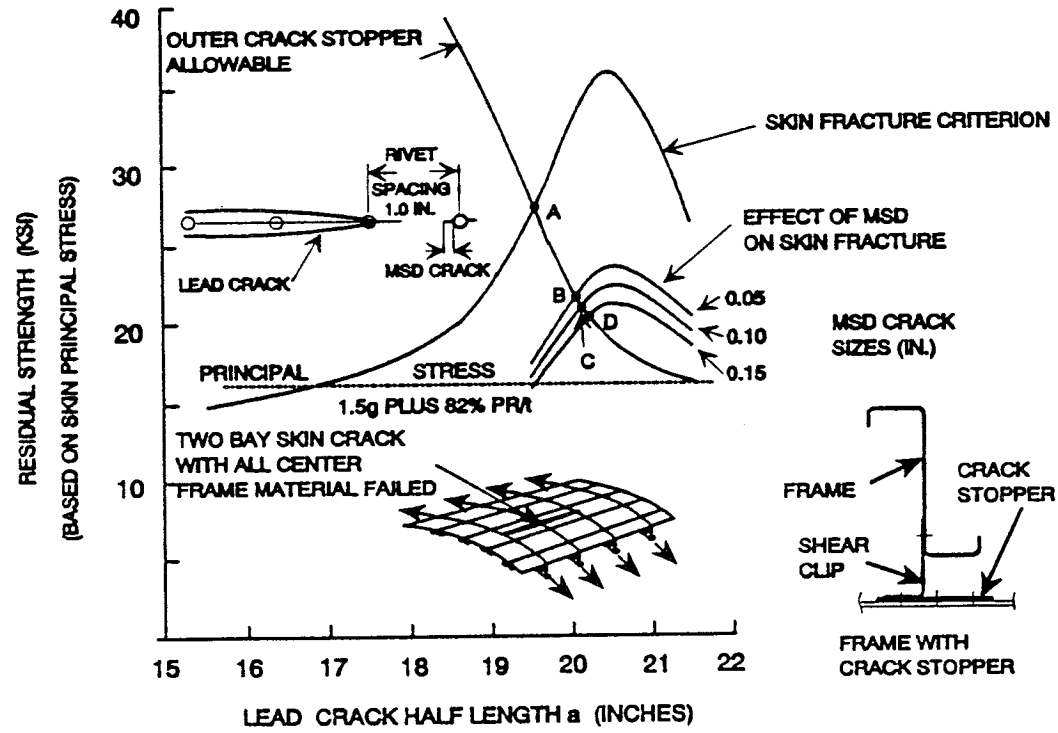

FIGURE 22 EFFECT OF MSD ON LEAD CRACK RESIDUAL STRENGTH
FRAMES WITH CRACK STOPPERS - RIVET SPACING 1.0 IN.

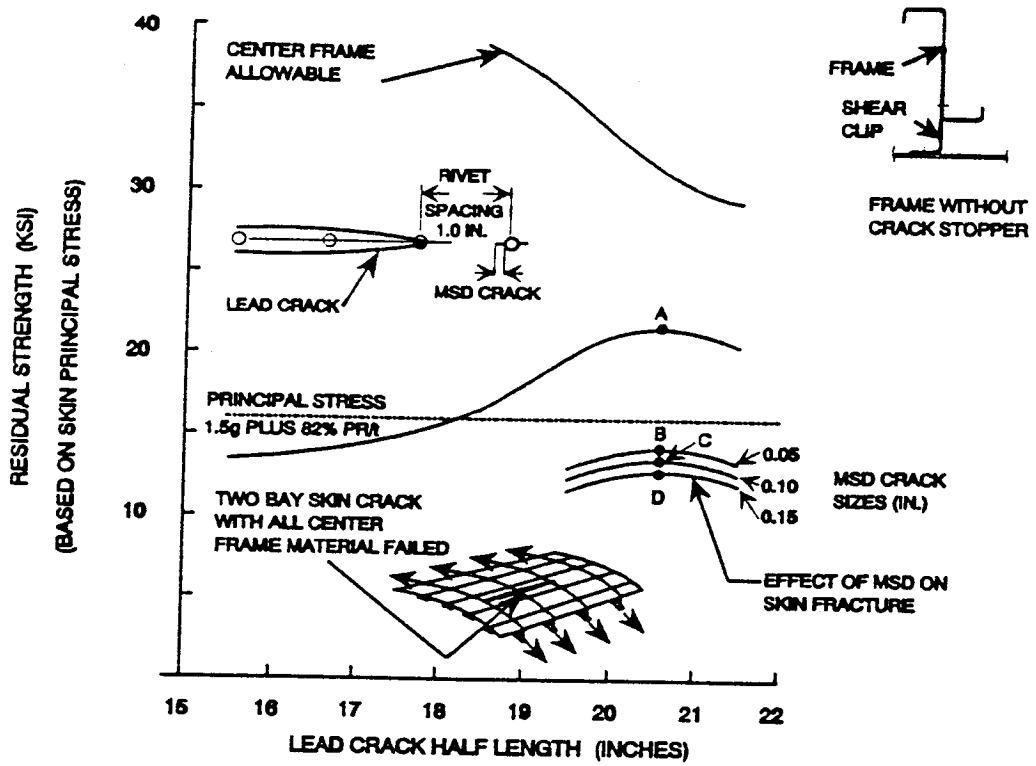

FIGURE 23 EFFECT OF MSD ON LEAD CRACK RESIDUAL STRENGTH
FRAMES WITHOUT CRACK STOPPERS - RIVET SPACING 1.0 IN.

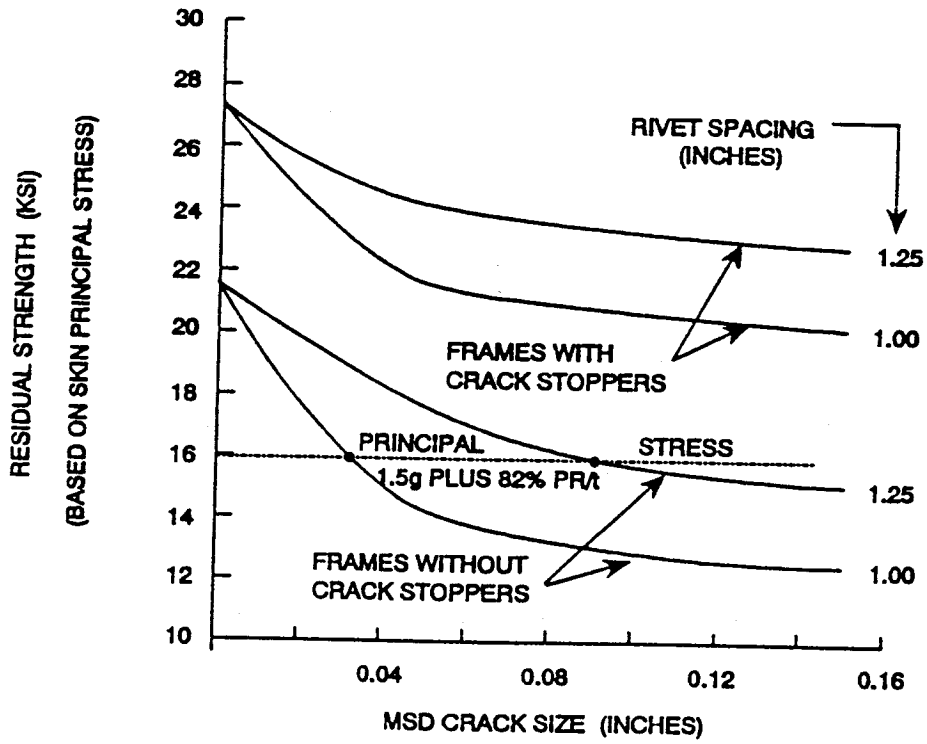

FIGURE 24 EFFECT OF MSD ON LEAD CRACK RESIDUAL STRENGTH FOR
TWO BAY LONGITUDINAL CRACK WITH BROKEN CENTRAL FRAME

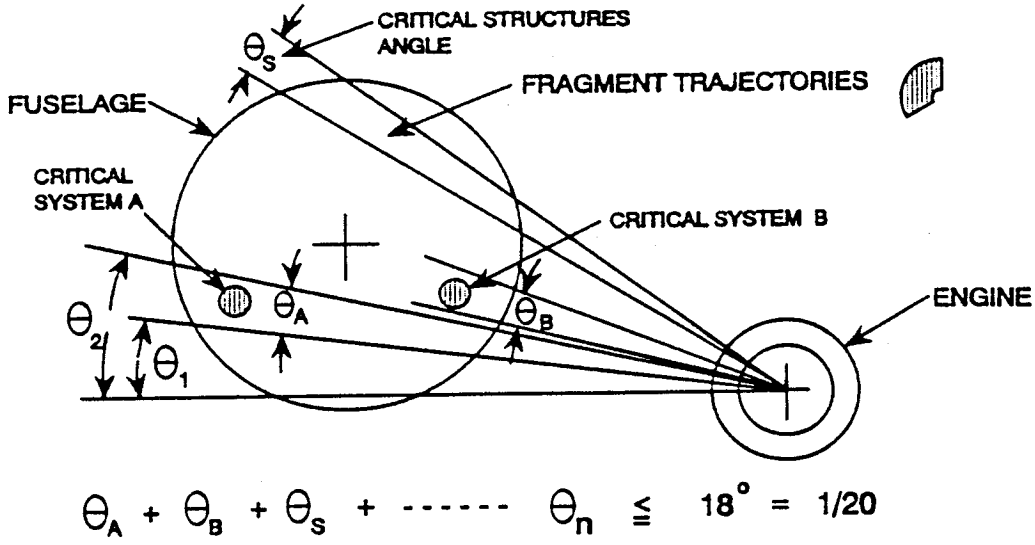

FIGURE 25 RISK EVALUATION - DISCRETE SOURCE DAMAGE

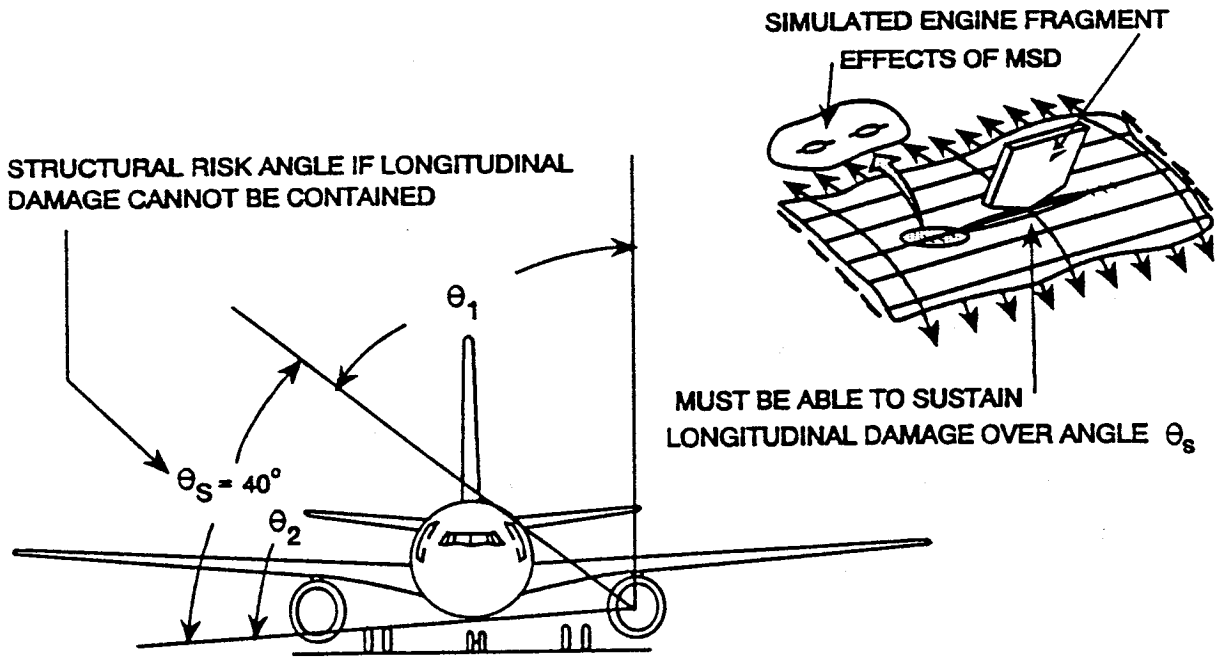

FIGURE 26 EFFECT OF MSD ON LONGITUDINAL DAMAGE CAUSED BY DISCRETE SOURCE DAMAGE MUST BE ACCOUNTED FOR IN ANY RISK EVALUATION

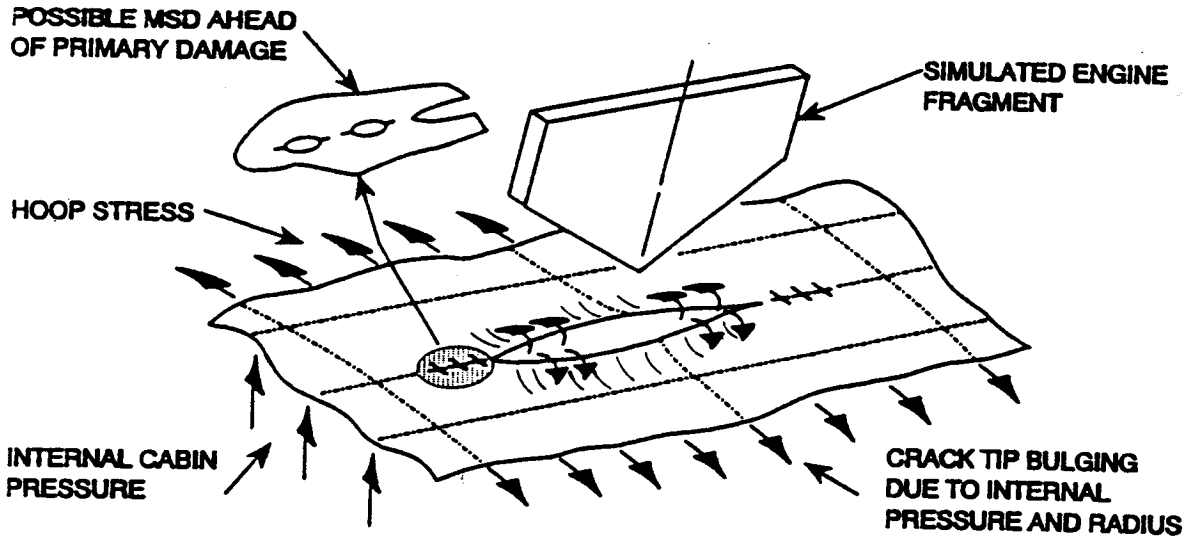

FIGURE 27 EFFECT OF MSD ON LEAD DAMAGE CREATED BY ENGINE FRAGMENT AT DAMAGE LENGTHS WHERE CRACK TIP BULGING DUE TO PRESSURE AND RADIUS IS HIGH

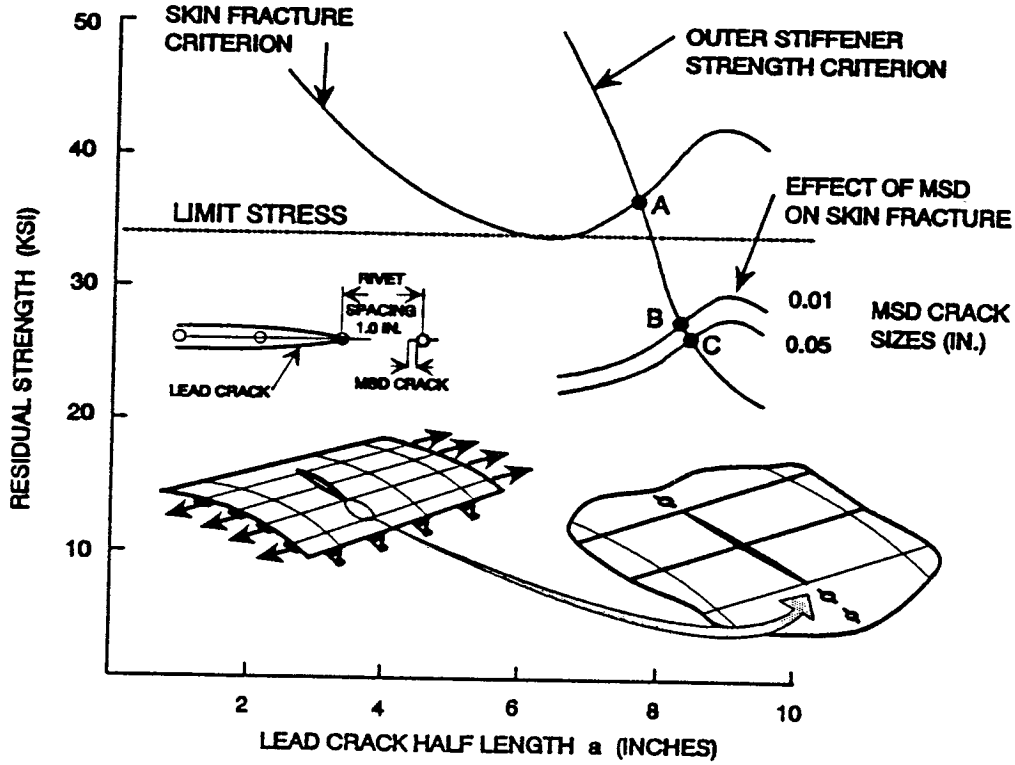

FIGURE 28 EFFECT OF MSD ON LEAD CRACK RESIDUAL STRENGTH TWO BAY CIRCUMFERENTIAL CRACK WITH BROKEN STIFFENER

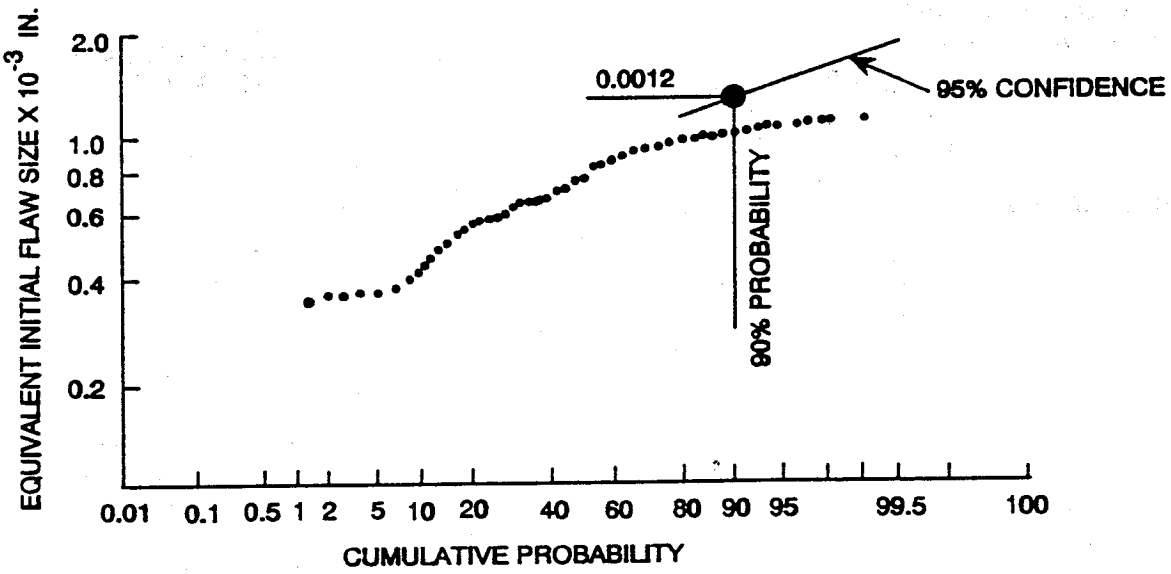

FIGURE 29 EQUIVALENT INITIAL QUALITY FLAW SIZE
EXAMPLE - REAMED COUNTERSUNK HOLES
TEST PANEL DATA

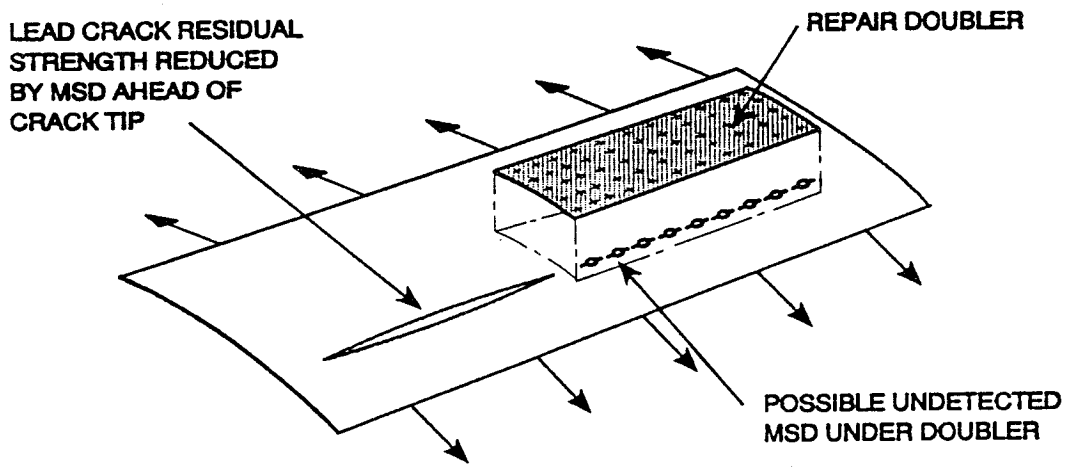

Figure 30 POSSIBLE LOSS OF LEAD CRACK RESIDUAL STRENGTH
DUE TO HIDDEN MSD UNDER REPAIR DOUBLER